Universidad de Oviedo

POLYTECHNICAL SCHOOL OF ENGINEERING OF GIJON

INDUSTRIAL ENGINEER IN ELECTRONICS AND AUTOMATICS DEGREE

FIELD OF ELECTRONICAL ENGINEERING

DC BUS HEALTH ESTIMATOR FOR POWER ELECTRONIC CONVERTERS

ALEJANDRO SALVADOR CABO
TUTOR: CRISTIAN BLANCO CHARRO

DATE: 28 JULY 2020

INDEX:

ABSTRACT

The breakdown of capacitors has been for many years a mind-bending issue in the renewable energy sector, different methods for good maintenance have being applied.

In this work the state of the DC link of Back-to-Back converters used in Doubly Fed Induction Generators of wind turbines will be estimated. An adaptive filter will be implemented to make the estimations with a determined period. Finally, with those estimations, an accurate tendency of the state of the capacitor will be obtained.

If this model is successful the downtime of wind turbine generators could be reduced as long as a preventive maintenance of the capacitor could be performed.

1. LIST OF ABREVIATIONS

WTG - Wind Turbine Generator

IG - Induction Generator

DFIG - Doubly Fed Induction Generator

DC - Direct Current

AC - Alternate Current

ESR - Equivalent Series Resistance

ESL – Equivalent Series Inductance

RLS - Recursive Least Squares

PMSG - Permanent Magnet Synchronous Generators

B2B - Back to Back

LS - Least Squares

kH - Kilohertz

MHz - Megahertz

mΩ - Mili Ohms

µF - Microfarad

EEPROM - Electrically Erasable Programmable Read-Only Memory

WIFI - Wireless Fidelity

VAT - Value Added Tax

2. INTRODUCTION AND SCOPE

Nowadays the importance of producing clean energy is a mind-bending point in the society, the climate change issue and all deaths caused by the pollution (air pollution contributed to almost 5 million deaths globally in 2017 [1]) are changing the way energy is produced.

Therefore, renewable energy is becoming one of the most important sources of energy. In Spain 36.8% of the electricity generated in 2019 came from renewable sources [2]. Where approximately 21% proceed from wind power generation. Currently there are 25.808 GW and new installation of 2019 was 2.319 GW [3].

While wind energy development shifting from onshore to offshore, the external environment where wind turbines are installed has become more and more harsh and therefore wind turbine components have to afford the meteorological conditions of those places. Therefore, its components are exposed in such environments and operate in varying wind for years, it is a big challenge to achieve predictable remaining lifetime, availability and maintainability. Considering the importance of this source of energy, an improvement of the efficiency of this energy production could be interesting in order to get better performance and therefore more energy.

As electrolytic capacitors used in the power converter systems of wind turbines have high failure and degradation rates among all of the components [4]. Estimating the life state of the DC bus of the power electronics that wind turbines incorporate will help to achieve a predictable maintenance for the capacitor, which, in turn, acts as filter between the converters of the Double Fed Induction Generator (DFIG).

Current techniques to check the remaining life of capacitors carry out the tests without any voltage applied on the capacitor, so wind turbines have to stop operating during the maintenance. However, the method proposed on this work will be able to make estimations during operations.

This work will focus on the DC link of the back-to-back converter used in Doubly Fed Induction Generator topology (DFIG) of wind turbines, as long as capacitor breakdowns are responsible of an important part of the wind turbines downtime.

Of course, there are different ways to calculate the lifetime of a capacitor, but none of them is precise enough and capacitors breakdown earlier or later than calculated due to the harsh and not predictable conditions where they work.

3. SPECIFIC OBJECTIVES

The main objective of this work is to develop a method to estimate the end of life of the capacitors placed in the DC bus of power electronic converters, more specifically in converters applied to DFIG. Thus, the capacitors can be replaced before they fail, avoiding non desirable stops.

The Capacitance and the Equivalent Series Resistance (ESR) associated to the capacitor will be estimated in order to check the state of life of the capacitor. This estimation will be done periodically even though the variation of the capacitor properties vary especially slow. Afterwards, those estimations will be compared with the critical values given by the capacitor manufacturer, in order to do a preventive maintenance and replace the capacitor before it breakdowns.

So as to achieve the estimations of the capacitance and the resistance, Recursive Least Squares (RLS) will be used. With this parametric identification method fast convergence to the real value is obtained.

A good state of capacitors will led into less problems of the rest of the power electronics since it reduces the current ripples and the peaks of voltage that go into the converters, so all the power converters will be healthier with a good state capacitor.

The low reliability of capacitors make this method interesting as checking the state of the capacitor periodically will lead into the knowledge on how the capacitor state is and their low reliability on these DFIG systems will not be a problem because it will be possible to substitute the passive component before any consequences may occur.

4. WORK METHODOLOGY

-First, some points were studied:

- Capacitor nature (How capacitors function).
- Parameters that affect capacitor lifetime and how they affect them (Temperature, current ripples, peaks of voltage).
- Which properties show the decline of Capacitor state (Decrease of capacitance and Increase of the associated resistance).
- Capacitor breakdown in power converters.
- Parametric identification methods.
- Recursive Least Squares method, and how to apply it to achieve the estimations that are needed.

-After these points were studied, next steps were followed:

- Modelling of the system.
- Model verification with theoretical data.
- Model simulation with experimental data.
- Comparison between theoretical and experimental data results in order to check the success of the model.

5. WIND TURBINES

The objective of wind turbines is the transformation of the kinetic energy of the air into mechanical power of the rotor blades. As the blades, when rotating have a huge torque due to the size and weight, its mechanical energy goes into a gearbox in order to multiply the number of turns. The output will be a rotor with less torque and higher rotational speed (the rotational speed of the double fed induction generators is commonly 1,000), which is easier to convert to electrical energy.

5.1 TYPES OF TURBINES

Depending on the position of the rotor axis, wind turbines are classified into vertical-axis and horizontal-axis ones:

-Horizontal axis: The horizontal axis wind turbine is a wind turbine in which the main rotor shaft is pointed in the direction of the wind. The rotor is located at the top of a tower where the winds have more energy and are less turbulent, this is the most common type of wind turbines, since it is more productive as it takes advantage of its height.

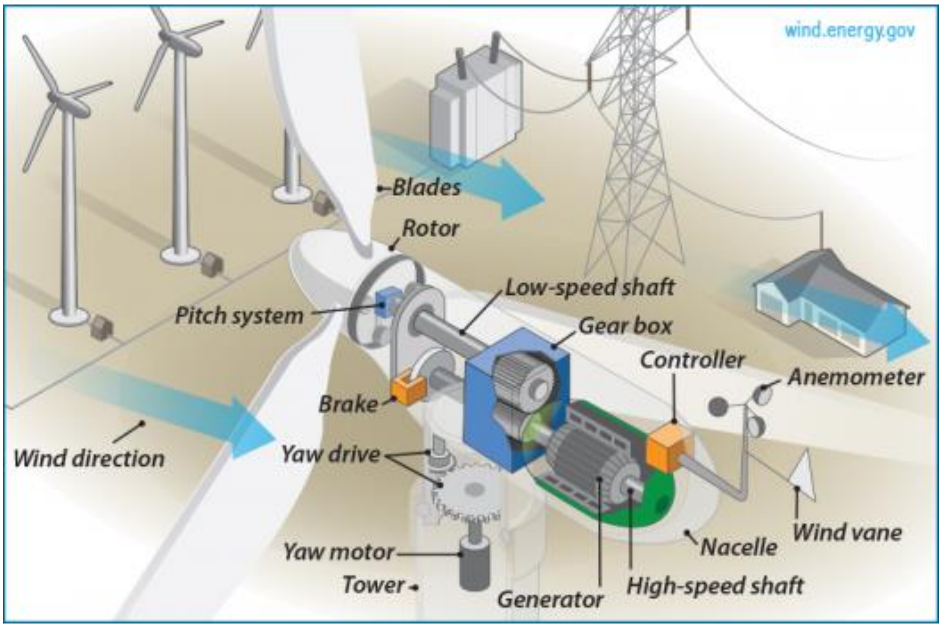

Figure 1. Horizontal axis Wind Turbine.[Office of energy efficiency & renewable energy]

The gearbox and the generator are located in a nacelle that is located at the top. There is also a yaw motor, which depending on the wind direction turns the rotor and the nacelle to point in the opposite direction of the wind. On the other hand, the power electronics are at the ground.

The pitch mechanism that is on the rotor is the responsible of turning the blades depending on the wind direction. When wind speed is very high, the control unit turns the blades in order not to move to prevent from damages as the turbines are designed for a determined wind speed range.

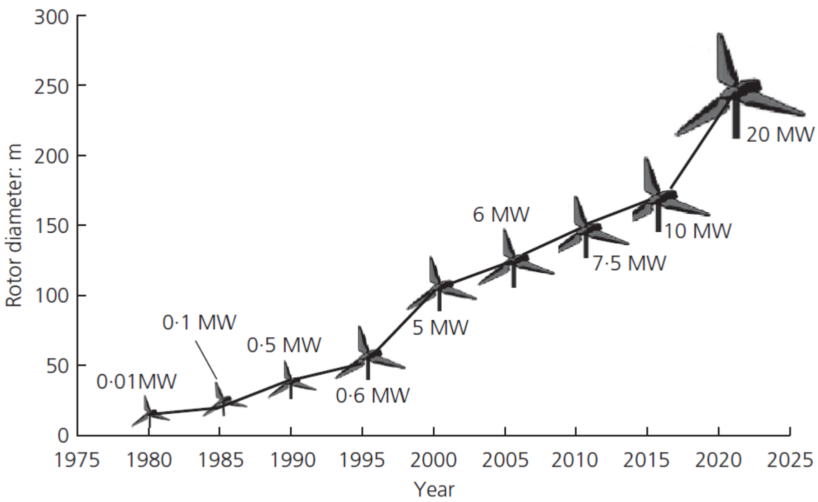

Figure 2. Wind Turbine energy generation compared with rotor diameter.

The production of energy per turbine has grown a lot over the last 30 years as seen in Figure 2, the improvement in the power electronics and the development of better controls of the turbines has permitted the use of bigger blades that perform more torque and therefore more mechanical energy.

-<u>Vertical axis</u>: A vertical axis wind turbine where the rotor is positioned transverse to the wind. Few vertical axis machines are available commercially, the main reason for this is that they do not take advantage of the higher wind speeds at higher elevations above the ground as well as horizontal axis turbines. The gearbox and the generator are located on the base of the turbine, which is an advantage when doing the maintenance or reparations.

In this case, as there is no orientation facing the wind, there is no need of yaw mechanism that turns the turbine and senses the direction of the wind, and there is no pitch mechanism either as the blades are fixed.[4]

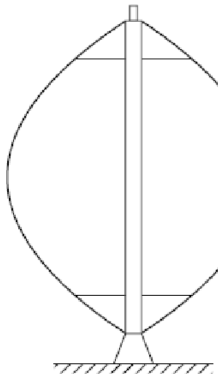

Figure 3. Vertical axis Wind Turbine.

5.2 TYPES OF TURBINES DEPENDING ON THE LOCATION

Apart from the type of turbines, WTG are also divided depending on where they are located.

This difference is because the land warms up in the sunny hours and gets cold by night. This variation in temperature implies a change in pressure too, considering this statement wind will blow from the sea towards the land during sunny hours, whereas at night, it will blow from the land towards the sea.

-Onshore

Onshore is said of WTGs, which are on the land.

Nowadays this is the most common way of producing wind energy being in Europe in 2019 about 90% of the power capacity of wind energy generation.

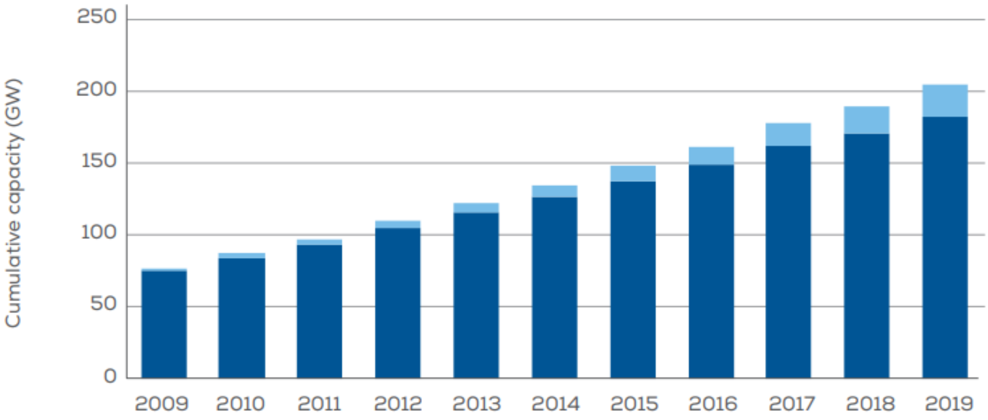

	2009	2010	2011	2012	2013	2014	2015	2016	2017	2018	2019
Offshore	2	3	4	5	7	8	11	13	16	18	22
Onshore	75	84	93	105	115	127	137	149	162	171	183
Total	**77**	**87**	**97**	**110**	**122**	**135**	**148**	**162**	**178**	**189**	**205**

Figure 4. Onshore vs Offshore Europe power capacity [3].

Onshore is cheaper to maintain and cheaper to construct, there is no need to consider waves, or sea impact in terms of degradation. Furthermore, the energy is developed closer to the grid and less energy losses are generated due to energy transport.

-<u>Offshore</u>

Offshore WTGs are located in the water, taking advantage of sea winds.

Offshore is still far from onshore power generation capacity, considering it is around 10% of the total capacity in Europe, being Europe the country with more offshore windfarms. Offshore is more productive as winds in the ocean are much consistent that winds on land, so less turbines are needed to produce same energy.

Moreover, the fact of being in the ocean is better as people are not affected by the impact they have on land. This may be the reason why countries like Denmark, which are small already change to offshore production. In 2019, the offshore newest generation in Denmark were higher than 90% compared with onshore.

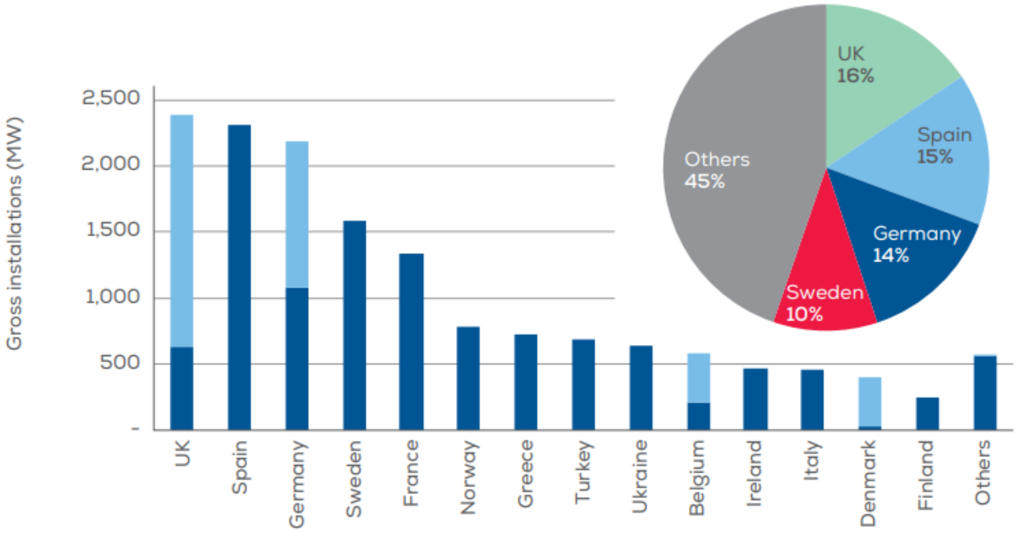

MW	UK	Spain	Germany	Sweden	France	Norway	Greece	Turkey	Ukraine	Belgium	Ireland	Italy	Denmark	Finland	Others
Offshore	1,764	-	1,111	-	-	-	-	-	-	370	-	-	374	-	8
Onshore	629	2,319	1,078	1,588	1,336	780	727	686	637	207	463	456	28	243	563
Total	2,393	2,319	2,189	1,588	1,336	780	727	686	637	577	463	456	402	243	571

Figure 5. European new WTG installations [3].

Vertical axis offshore WTG could be also considered as the centre of gravity is much lower compared with horizontal axis and therefore bigger blades and higher capacity could be achieved, since the stability is one of the main problems when installing offshore WTG.

Offshore turbines depending on how deep is the water where they are installed can be divided into:

-Shallow water: < 40 meters depth

-Transitional water: Between 40 and 60 meters depth

-Deep water: > 60 meter depth

Different installations are made depending on the depth, the deeper the more complex the system has to be.

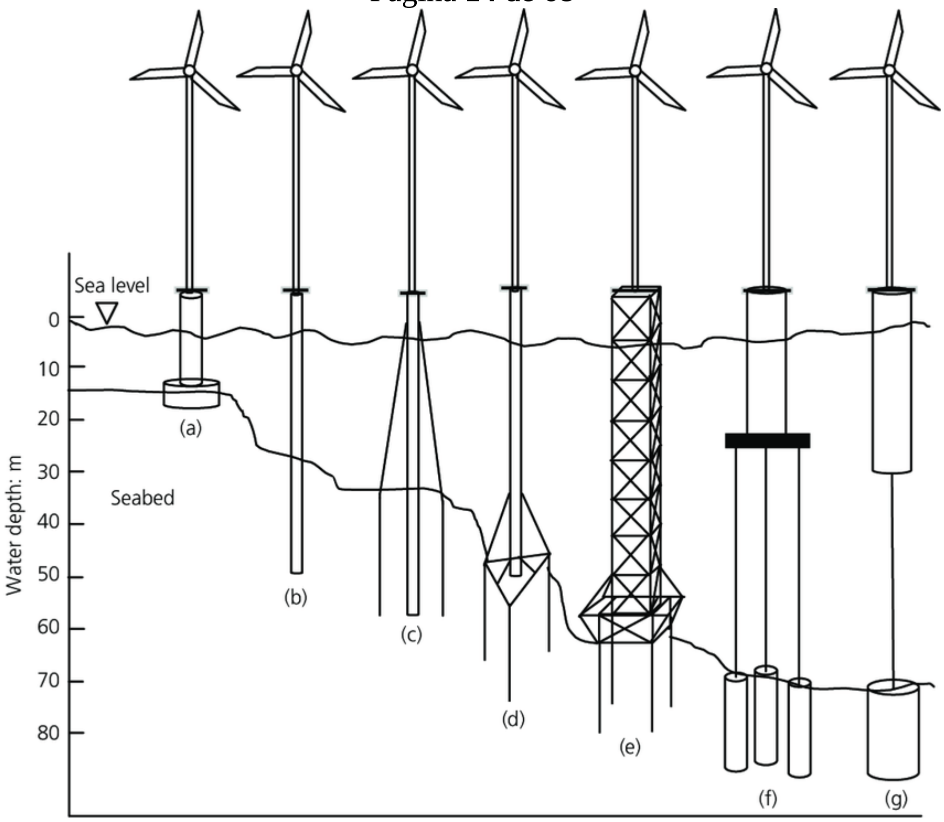

Figure 6. Different structure options for Offshore WTG (a) gravity; (b) monopile; (c) monopile with wires; (d) tripod; (e) braced frame; (f) tension leg with suction buckets (ballast stabilised); (g) buoy with suction anchor [5]

6. POWER CONVERTER TOPOLOGIES FOR WIND TURBINE GENERATORS

Different topologies are used in wind generators. Since each generator has associated some needs, depending on the type of generator the power converter topology will change in order to get the highest efficiency as possible.

There are two types of generators used in turbines:

-Synchronous generators.

A synchronous generator is a machine whose generated voltage waveform is synchronized with the rotor speed. The magnetic field of the rotor is supplied by direct current or permanent magnets.

$$frequency = \frac{\text{Synchronous speed (rpm)}\ x\ nº pole\ pairs}{60}; \qquad \text{(Eq. 1)}$$

This means that slip between stator and rotor is zero, therefore the efficiency of synchronous generators is higher than for the asynchronous.

-Asynchronous (induction) generators.

In contrast with synchronous generators, asynchronous generators have higher frequency as there is some slip between the generated voltage waveform and the rotor speed.
The magnetic field of the rotor is supplied by the stator through electromagnetic induction.

$$frequency > \frac{\text{Synchronous speed (rpm)}\ x\ nº pole\ pairs}{60}; \qquad \text{(Eq. 2)}$$

Both of them have some advantages and disadvantages, but asynchronous generators are more common in the industry since they are relatively cheap, and they need lower maintenance.

6.1 PERMANENT MAGNET SYNCHRONOUS GENERATORS

Permanent magnet Synchronous Generators (PMSG) are mainly used in smaller turbine types, since this kind of configuration develop higher efficiency in addition to smaller wind generator blade diameter.

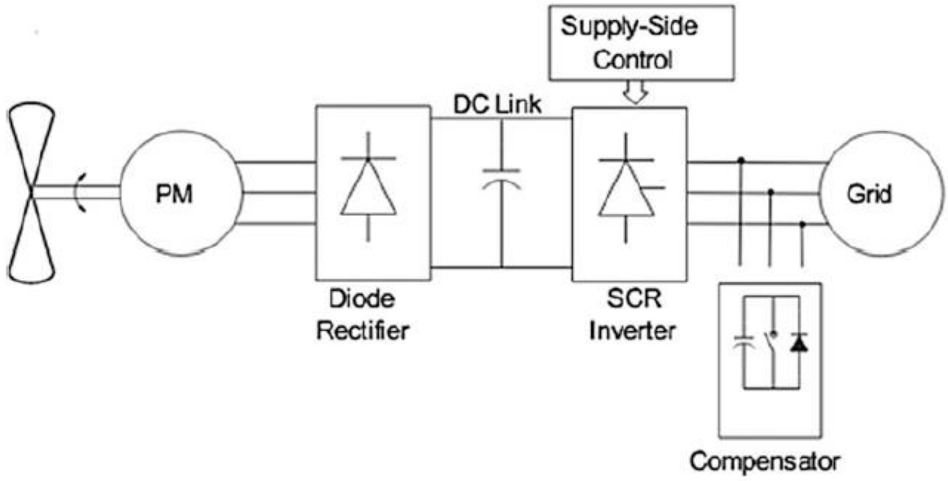

Figure 7: PMSG topology

One of the benefits that presents PMSG configuration is that they do not require from external excitement current. The fact of not having external excitation allows to use a diode bridge rectifier instead of a back to back converter, since current flow is not needed in both directions.

As shown on Figure (7), a thyristor inverter is used at the grid side in order to have a continuous control on the inverter working angles, controlling the rotor speed is possible with the DC voltage, hence, is possible to have high efficiency.
Furthermore, this configuration includes lower device cost and reduced power losses compared with hard switching inverters.

Obviously, there is also a drawback in PMSG topology, the need of an active compensator for the reactive power demand and for the reduction of the harmonic distortions.
Moreover, this kind of generator is more expensive and the maintenance is more intensive too. [6]

6.2 INDUCTION GENERATORS

Since inductor generators (IG) require external reactive power control from the grid, the generator´s side power converter must let current flow in both directions.

Therefore, it is important to understand the back-to-back (B2B) converter topology.

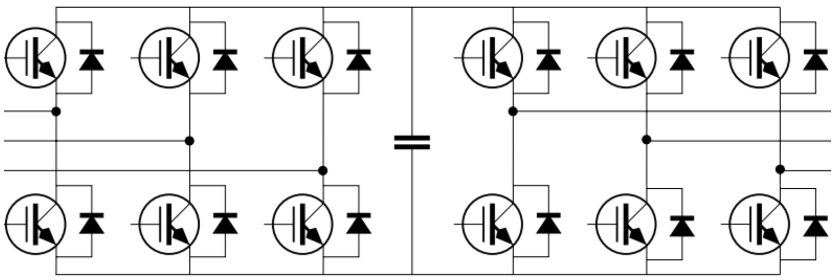

Figure 8. Back-to-Back converter

As shown on Figure (8), this topology is formed by two full bridge converters of six switches each. The operation of the B2B converter consists in two decoupled converters rotor side and grid side in which the amplitude, phase and frequency can be controlled independently from each other.

Both converters can work in two different modes, active rectifier mode and inverter mode:
-Active rectifier: When the converter works on this mode the energy is transferred to the left side of the converter, this is how the reactive power is controlled.

-Inverter: On this case, the transfer of energy is to the right.

With these modes, the B2B converter is able to transfer energy in both directions when is needed.
To control the B2B converter Pulse With Modulation (PWM) is implemented and therefore the amplitude, the phase and the frequency are controlled and both modes can be developed to achieve the needs of the IG.
In Figure (9). it is shown a simple inductor generator, where the B2B converter is used.

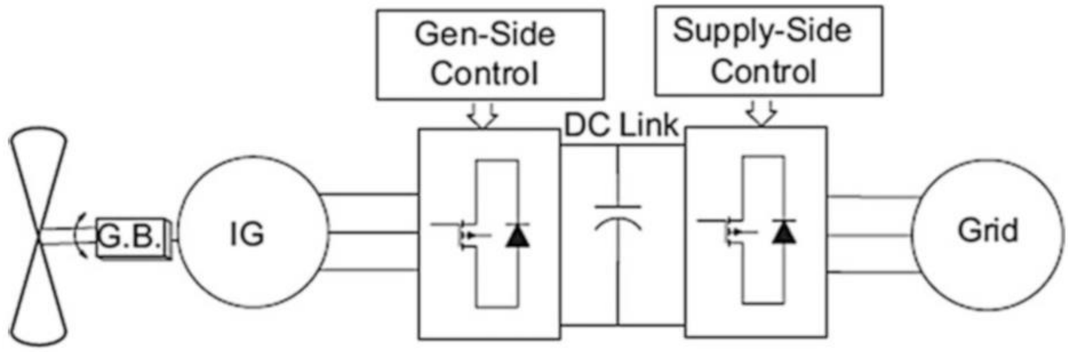

Figure 9. Simple inductor Generator topology

When the generator side converter delivers power to the DC link, the DC voltage of the DC link increases, therefore the rotor side converter has to give power to the grid, as the grid voltage is fixed the grid side converter delivers current to the grid in order to keep the voltage of the DC link constant. To do this, the grid side converter generates an AC voltage in phase with the grid voltage one.

This topology is used in fixed-speed wind turbines, as the generator output is connected to the grid the speed of the generator rotor is fixed, obviously with some margin but there is no possibility of rotor variable-speed. Therefore, when the speed of the wind increases this kind of topology is not able to optimize power generation.[7]

7. DOUBLY FED INDUCTION GENERATOR

The DFIG is also an induction machine with a wound rotor, which main difference with the simple induction generator is that both, the stator and the rotor are electrically connected. Although the nature of the DFIG indicates that it is an induction generator machine, its fundamental of operation is similar to a variable speed synchronous generator.

This work is focused on the DC link of the B2B converter used in DFIG wind turbine systems.

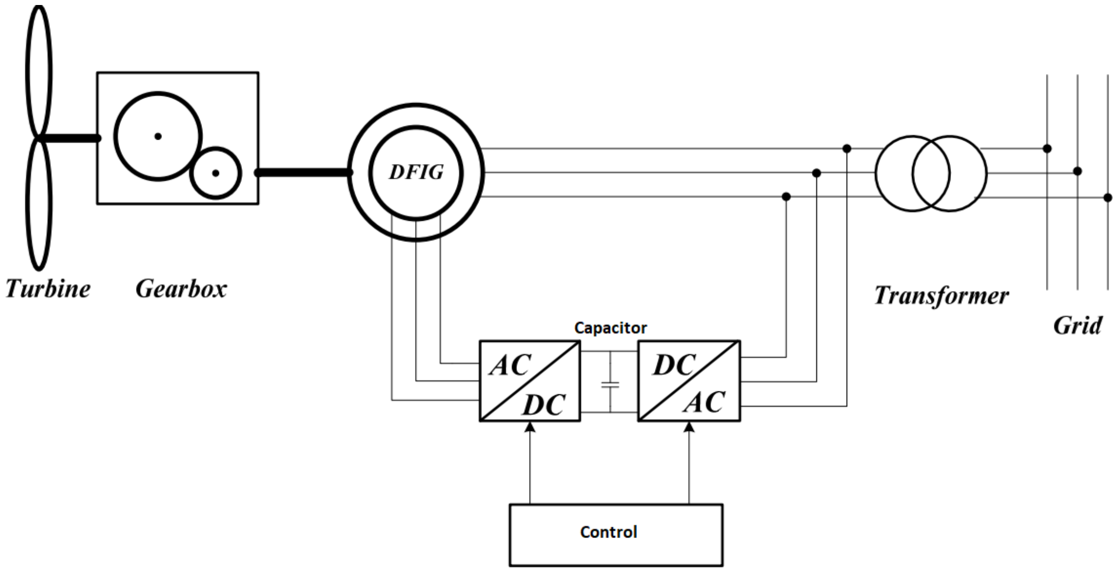

Figure 10. DFIG simplified electrical diagram.

A back-to-back converter is included as shown at Figure (10). The power electronic converters need only to handle a fraction of the total power. The rotor power is typically about 30% nominal generator power. Thus, the rest of the power is delivered directly to the grid from the stator.

Therefore, the losses in the power electronic converter are reduced, compared to a system where the converter has to handle the entire power, this is the reason why the system cost is lower too compared with simple IG.

A Maximum Power Point Tracking control strategy is implemented on DFIG in the range of wind speeds allowed, by controlling the electromagnetic torque of the generator. The mechanical torque that is determined by the blades torque and electromagnetic torque, makes the rotational speed of the machine fit to a reference value in order to maintain an optimal tip-speed-ratio, and therefore have higher efficiency.

The electromagnetic torque of a DFIG is controlled by the rotor current. For a DFIG rotor associated with a B2B converter and with the stator directly connected to the grid, the scheme controls the active and reactive power on the stator side separately. This requires the measurement of stator and rotor currents, stator voltages and rotor phase angles.

The rotor current is controlled by the control unit to achieve the reference of active and reactive power. With the different measurements made, the control unit is able to determine the rotor reference voltages and then the switching signals for IGBTs to produce the required voltages for the B2B converter.

DFIG machine has two different working modes depending on the rotor speed:
-When the rotor speed is higher than the electrical synchronous speed of the stator, the rotor delivers energy to the grid, this mode is called super-synchronous generating mode.

-On the other hand, when the rotor speed is lower than the electrical synchronous speed of the stator, the grid is delivering energy to the rotor, whereas the stator continues delivering energy to the grid, this mode is called sub-synchronous generating mode.

Therefore, the DFIG has the ability to rotate over a wide range of speeds. However, keeping the control of the voltages and currents of the generator´s rotor allows it to keep synchronised with the grid when the wind speed varies.

DFIG controls the magnitude and angular position of the rotor flux to regulate the real and reactive power. This is necessary to keep the stability of the system.

In conclusion, the main advantages of the doubly fed induction generator compared with the induction generator are:
-It is possible to keep the amplitude and the frequency of the voltage constant even though the wind speed is changing.
-Even with low wind speeds, electrical generation is possible.
-As DFIG is more efficient, the power generation for same wind speeds is improved.
- The major benefit from the DFIG is that it offers separate real and reactive power control, almost like a regular synchronous generator, even though running asynchronously. This

is because the industry has matured the ideas of vector or field oriented control over induction machines.

Using these control techniques, the torque providing components of this rotor flux can respond fast enough to keep the application under control, even for the duration of significant grid disturbances.

This is the reason why, the DFIG is one of the most used configurations in the wind industry, having different advantages such as low cost and complexity, requiring a low converter capacity, and decoupling of active and reactive power control.

The DFIG is currently the system of choice for multi-MW wind turbines. The system must be able of operating over a wide range of wind speed in order to achieve optimum efficiency. Therefore, the rotor of the generator must be able to operate at a variable rotational speed. The stator circuit is directly connected to the grid while the rotor winding is connected to a three-phase converter. [8] [9] [10] [11]

8. CAPACITORS

Capacitors belong to the passive components as resistors and inductors. Capacitors are composed of two electrical conductors, the anode and the cathode, separated by an insulating layer, the dielectric.

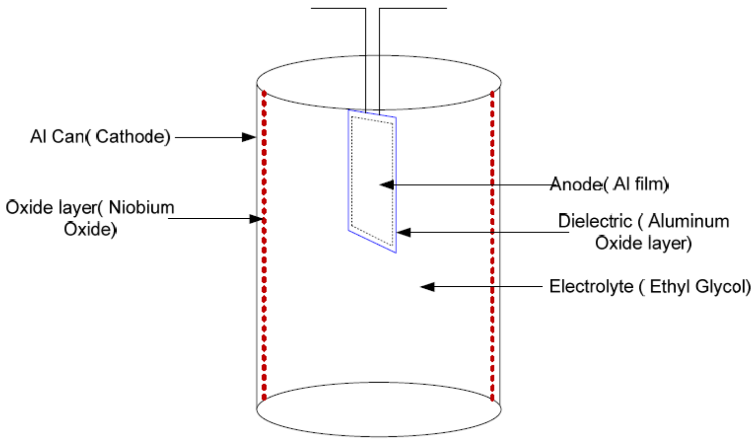

Figure 11. Capacitor

Capacitors are able to store energy, the energy is stored by charge separation between the two conductors. The amount of charge stored (capacitance) depends on:

- Size of the plates (conductors)
- Properties of the dielectric material that separates the conductors
- Distance between the plates

$$\text{Capacitance} = \frac{Permitivity\ of\ the\ dielectric\ \ x\ Area}{Distance}; \qquad \text{(Eq. 3)}$$

Depending on the capacitance, they have different applications, low capacitances are principally used to couple signals, whereas high capacitances are mainly used to protect power systems.

There are different types of capacitors, the most common are:

- Electrolytic Capacitor
- Ceramic Capacitor
- Mica Capacitor

8.1 TYPES OF CAPACITORS USED IN POWER SYSTEMS

In power applications, as current and voltage are high, capacitors with a high capacitance are needed. Therefore, focus will be on capacitors with this characteristic.

Electrolytic capacitors main characteristic is their much higher capacitance per unit volume, this is due to their reduced dielectric oxide layer and enlarged anode surface. However, they are sensitive to temperature, frequency and have low reliability.

Electrolytic capacitors use a chemical feature, which on contact with a particular electrolyte form a very thin insulating oxide layer on their surface by anodic oxidation.

Electrolytic capacitors must work with higher voltage at the anode than at the cathode, if this statement is not fulfilled the capacitor may explode or simply break.

The three groups of electrolytic capacitors are:

-Aluminium electrolytic capacitors with aluminium oxide as dielectric.

There are a wide variety of sizes, so this type of electrolytic capacitors are suitable for many applications.

-Tantalum electrolytic capacitors with tantalum pentoxide as dielectric.
The permittivity of tantalum pentoxide is approximately three times higher than aluminium oxide. It is a good option when there is no space available. Therefore, this group is basically used in electronic devices and in military industry.

-Niobium electrolytic capacitors with niobium pentoxide as dielectric, Niobium is not even comparable to Tantalum as their properties are almost the same, this type of capacitors became popular because they were cheaper than Tantalum.

Aluminium electrolytic capacitors are the cheapest and most used in electronics.

9. CAPACITOR FAILURES AND REASONS OF FAILURE

Know the type of failures that might be produced in a capacitor and its reasons is important, as long as this work implements a method to minimize capacitor failures.

Failures of capacitors are of two types:

-Catastrophic failures
There is a complete loss of functionality due to a short or open circuit, or there is a breakdown or explosion of the capacitor due to excessive internal pressure.

-Degradation failures
There is gradual deterioration of capacitor function.
Failures could also be divided into three groups depending on when along its lifetime they fail, they follow a bathtub curve failure rate like:

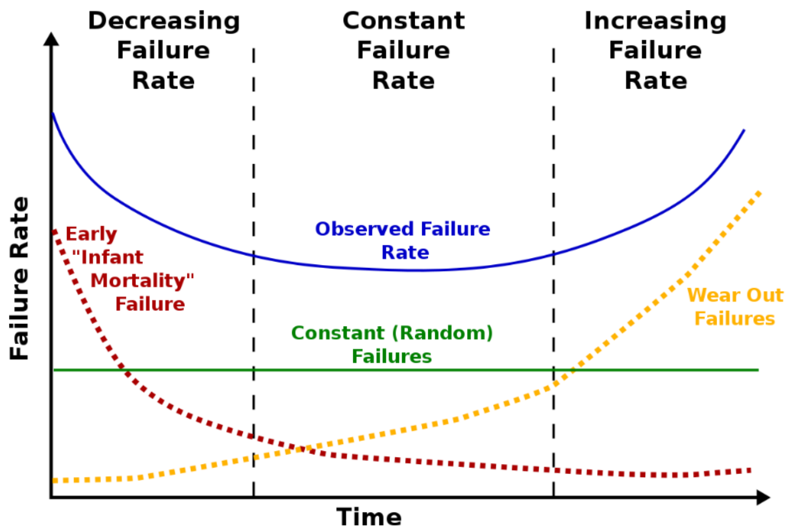

Figure 12. Bathtub curve

-Early failure period

Early failures in capacitors are due to deficiencies in design or manufacturing process or incompatibility with operation conditions. Sometimes these early failures are also due to human errors i.e., positioning the cathode or the anode the other way.

This period is included in catastrophic failures.

-Random failure period

The failure rate on this period is low, this kind of failures are unexpected, since this period is before its estimated life.

This period is part of catastrophic failures too.

-Wear-out failure period

In this period, the failure rate gets higher with time as the degradation starts to be significant.

This period is included in degradation failures.

However, this kind of failure could instead become a replacement, if the implemented model of this work is successful.

9. 1 PARAMETERS THAT AFFECT ELECTROLYTIC CAPACITOR LIFETIME

Electrolytic capacitors lifetime is not fixed, but it depends on the application conditions:

- Ambient parameters: Temperature, humidity, atmospheric pressure and vibrations.
- Electrical parameters: Voltage of operation, ripple current and charge-discharge rate.

In spite of the fact, all these parameters affect capacitor lifetime, ambient temperature and heating due to the electrical parameters (ripple current and operating voltage) are more significant and critical to determine the longevity of the capacitor.

A chemical reaction occurs within the capacitor where the dielectric materials deteriorate. This chemical reaction may cause that the dielectric material does not support the applied voltage as it is reducing its properties during time.
The speed of this reaction depends on the temperature as follows:

Formula considering Arrhenius law, to get the lifetime of an electrolytic capacitor:

$$\boldsymbol{L} = \mathbf{L0} \text{ x } \mathbf{2}^{\frac{(\mathbf{T1-T2})}{\mathbf{10}}} \qquad \text{(Eq. 4)}$$

L: Expected lifetime (hours)

L0: Lifetime under maximum rated operating temperature (hours)

T1: Allowable maximum temperature

T2: Temperature of operation

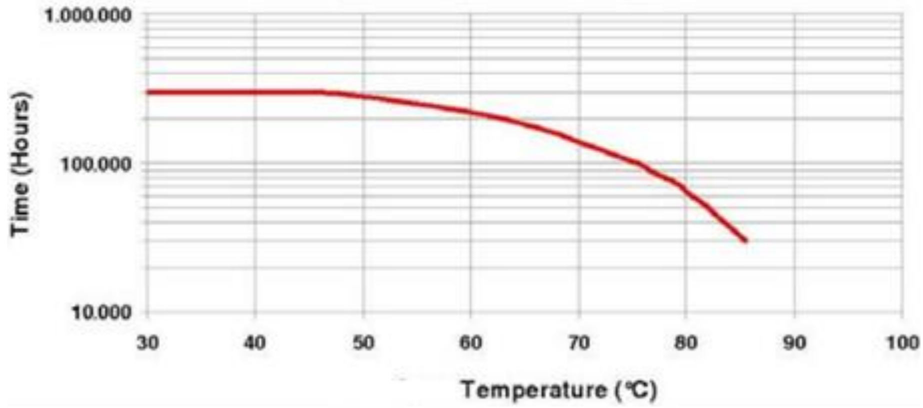

Figure 13. Capacitor lifetime vs Temperature

Considering the formula, with every ten Celsius degree drop, the life of the capacitor will double as shown at Figure (13), where the lifetime is being compared with the temperature.

The problem comes from the fact, the estimation with that formula is not precise because the temperature depends on different factors, which are not easy to estimate either because a simple small change on the temperature on operation could make a huge change on the final result of the lifetime. This is why electrolytic capacitors are not reliable.

Obviously, there is a temperature range where this formula works, but if the temperature becomes higher and stays far from the supported temperature of the capacitor for a long period of time a catastrophic failure may occur.

Apart from the chemical reaction where the dielectric gets reduced, there is another way for capacitors to deteriorate, it is related with the leakage current, even though dielectric materials are supposed not to let pass any current, there is always a little amperage through the dielectric when voltage is applied between the two poles of the conductor. Despite the current being almost null, this leakage current produces some localized heating and electron interactions.

The capacitor degradation brings the loose of its main electrical parameters getting a bigger ESR and a smaller capacitance.

The consequences that happen when the following phenomenon occur are:

-High voltage applied at the capacitor: The capacitance decreases and ESR increases.

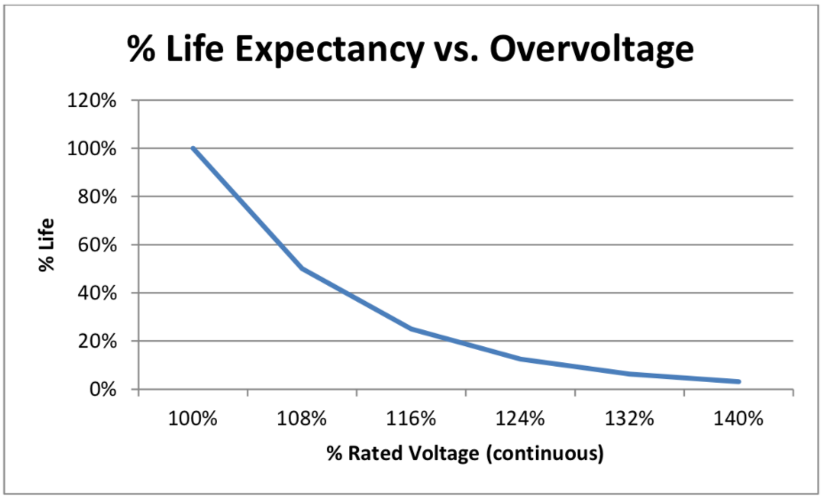

Figure 14. Life expectancy vs Overvoltage [PQMC, Causes of Premature Failure of Power Factor Capacitors]

-Transients: The leakage current could become high and an internal short-circuits may occur too.

-Reverse bias: The leakage current gets higher.

-Vibrations: When vibrations occur internal short circuits, capacitance losses, leakage currents, increase in ESR and even open circuits may happen.

-High ripple current: Internal heating is caused when high ripple current appears, increasing the core temperature.

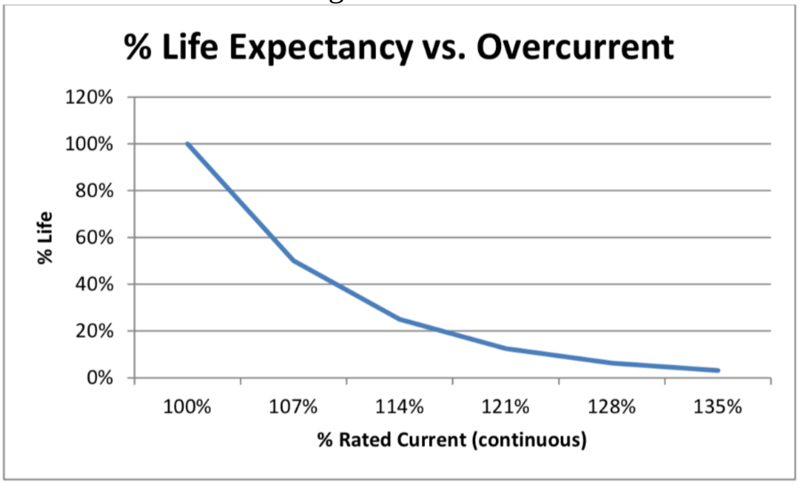

Figure 15: Life expectancy vs Overcurrent [PQMC, Causes of Premature Failure of Power Factor Capacitors]

The internal power dissipation (heating) produced by the ripple current can be expressed like:

$$P = \text{Iripple}^2 \text{ x ESR} \qquad \text{(Eq. 5)}$$

Where

P – Internal power dissipation

Iripple- Ripple current

ESR- Equivalent series resistance

With the degradation of the capacitor, the ESR is increasing and therefore the power losses are more significant, that is why the degradation is making the lifetime reduce exponentially.

Therefore to get the increase of temperature:

$$\Delta T = \frac{\text{Iripple}^2 \text{ x ESR}}{\text{K x A}} \qquad \text{(Eq. 6)}$$

Where

ΔT - Temperature rise

K - Heat transfer [W/m^2 x Kelvin]

A - Surface area

Equilibrium temperature will be found when numerator and denominator are equal.

If the capacitor operates below their rated voltage then the component will be under less operating stress and lower leakage current, which provides an improvement in life expectancy, therefore if the capacitor is well selected degradation may be slow enough so it needs careful consideration.[12] [13]

9.2 CRITICAL VALUES OF CAPACITORS

Since DFIG capacitors have low reliability, their critical parameters must be checked to know how reliable the capacitors are and be able to replace them before they breakdown.

The health of the capacitor is commonly measured by the ESR value. The ESR of the capacitor is the sum of the resistance due to the oxide (aluminium), electrolyte, spacer, and electrodes.

Over the operating period, the capacitor degrades, its capacitance decreases and ESR increases. Depending upon the percentage increase in the ESR values and the capacitance we can evaluate the healthiness of the capacitor. There are certain industry standards for these parameters, if the estimations of the model exceed these standards then the component is considered failed and should be immediately replaced before further operations.

The following statements will be compared with the results obtained using our model:

For capacitors rated between 40 Volts and 160 Volts [14]

DC ΛC/C > ±20%

ESR> 3x initial limit

Leakage Current > specified amount in datasheet

The voltage applied in the DC link of the B2B in the experiments is over 160 volts, so the critical parameters are the following:

For capacitors rated above 160 Volts

If one of these statements is true, capacitors life got to its end:

DC ΛC/C > ±15%

ESR> 3x initial limit

Leakage Current > specified amount in datasheet

10. THE IMPORTANCE OF THE COOLING

In the power generation process, power losses are dissipated as heat, which directly influences the efficiency of the generator, and the temperature rise due to heat dissipation will further lower the power generator efficiency. In addition, the temperature rise within a generator will accelerate the insulation ageing and therefore affect the life of the generator.

However, the problem that affects the capacitor is the heat in the power conversion system, thus focus will be on this part.

Heat has a known detrimental impact on many power conversion components including capacitors, IGBTs, and printed circuit boards as it was shown in [9. 1 PARAMETERS THAT AFFECT ELECTROLYTIC CAPACITOR LIFETIME

Considering this equation, it is seen how important is a good refrigeration to keep the capacitor lifetime and reduce the degradation process as much as possible.

$$\Delta T = \frac{\text{Iripple}^2 \text{ x ESR}}{\text{K x A}} \qquad \text{(Eq. 7)}$$

, where

ΔT - Temperature rise

Iripple- Ripple current

ESR- Equivalent series resistance

K - Heat transfer [W/m^2 x Kelvin]

A - Surface area

When designing a cooling, it is necessary to get a denominator that is higher or equal than the nominator during more than half of the time of operation, then, the temperature will get reduced or keep constant, as long as, the higher the value of the heat transfer rate the lower the temperature rise.

In this part, the parameters that must be taken into account when making a design of a cooling, and, different cooling methods will be seen.

As turbines need wind to work, many factors need to be considered when designing the refrigeration system as it will deal with outdoor meteorological conditions. When dealing with outdoor environments, heat is particularly problematic as the operating environment could have a high ambient temperature and powerful solar radiation.

In the world of high power electronics, there are different cooling methods. These methods include air-cooling, liquid cooling, heat pipes, etc.

The design of a good cooling needs careful consideration of several factors including design cost, desired operating life, ease of maintenance, and operating environment when choosing one of those cooling methods.

-Air-cooling works properly for low power applications, but it is not suited for high power applications, since air is a good insulator, but is not ideal for removing heat.

-Liquid cooling techniques for power module are mainly divided into indirect cooling and direct cooling.

- Indirect cooling means that the power module is assembled on a closed cooler through a thin layer of thermal interface material (e.g. cold plate). This works with the liquid flowing inside the cold plate, it is usually propelled by a pump, it makes the liquid flow in a cycle where it removes heat from the converter and later it gets rid of that heat before going back to the cold plate to remove the heat again.

- On the other hand, direct cooling means that the coolant is in direct contact with the surface to be cooled, which is often done by pin fin designs. Direct liquid cooling eliminates the layer of thermal interface material that is between the power module and the cold plate. [15] [16]

11. IDENTIFICATION OF SYSTEMS

In this part of the project the identification of systems will be seen, systems can be represented in a simplified way using a model.
Models allow experimentation on it for the prediction and control of system behaviour, and this allows to avoid experimentation on the real system, which sometimes is complicated or just too expensive.

11.1 SYSTEMS

Before going into detail about the concepts related to the identification of systems, it is necessary to clarify some terms that will be used during the project.

The first thing to consider is the concept of the system.
A system is a set of elements that act together to achieve an objective. Systems provide controlled signals, output (“y”), from signals that can be manipulated, inputs (“u”). The

outputs of a system can also be modified by the disturbances, which are unmanageable and unwanted signals (“e”).

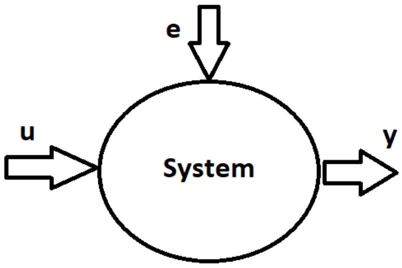

Figure 16. System

Systems can be found in open loop or closed loop. The output of open loop systems is not compared to the value of the input signal.

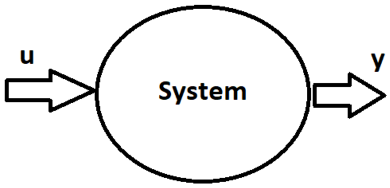

Figure 17. Open loop system

On the other hand, in closed loop systems, the output, in order to be controlled, is compared to the signal of reference, The system knowing the input (signal wanted) and the output (signal obtained) is able to vary the input to get the desired output.
Closed loop systems are useful when disturbances are difficult to predict.

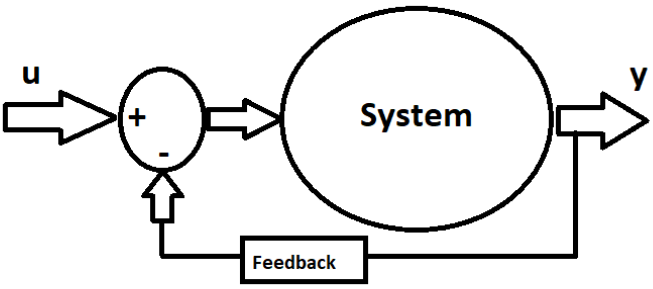

Figure 18. Closed loop system

11. 2 PARAMETRIC OR MATHEMATICAL MODELS

Depending on the type of system and the mathematical representation used, the systems are classified like:

First:

- Deterministic: Deterministic means the results are predictable, there is a tolerance limit in the results, in other words, there is not randomness associated. This means, that it could be possible to define the relation between inputs and outputs with an equation.

- Stochastic: There is randomness associated, the results are not predictable, instead of be defined by an equation are defined by probability models.

Second:

- Static: A system is said to be static when the output depends directly from the input, there is not change in the output with time.

- Dynamic: The outputs vary with time after an input is applied to the system.

Third:

- Continuous: The signals or variables of the dynamic systems are a function of time. Continuous systems work with continuous signals over time, and their model is characterized by differential equations.

- Discrete: systems work with sampled signals, where time is divided into periods of constant value. Discrete models are useful, when past samples need to be used in the model. For example a signal X at the instant n-2 is needed as input in the model.

11. 3 PARAMETRIC IDENTIFICATION MODELS

Some famous models are:

-AutoRegresive with eXogenous input (ARX)

This model is built with data measured of input and output of a system, the behaviour of the system can be represented with two vectors called input regression size n + 1 and output regression size n.

The coefficients "aj" and "bj" are the parameters to be estimated applying a numeric analysis technique.

This model works for the multivariable LS.

$$\mathrm{y(k)} = \sum_{j=1}^{n} a_j \mathrm{y(k\text{-}j)} + \sum_{j=0}^{n} a_j u(k-j) + e(k), \qquad \text{(Eq. 8)}$$

in other words:

$$y_k = -a_1 y_{k-1} - \ldots - a_n y_{k-n} + b_1 u_{k-1} + \ldots + b_n u_{k-n} + e_k \qquad \text{(Eq. 9)}$$

where "e_k" is random noise.

-AutoRegresive Moving-Average with eXogenous input (ARMAX)

Less specific than the ARX model, but it does not work for the multivariable LS identification.

$$y_k = -a_1 y_{k-1} - \ldots - a_n y_{k-n} + b_1 u_{k-1} + \ldots + b_n u_{k-n} + e_k + c_1 e_{k-1} + \ldots + c_n e_{k-n} \qquad \text{(Eq. 10)}$$

, where “e_k” is random noise.

- AutoRegresive Moving-Average (ARMA)

This model is divided in two parts the autoregression part (AR) and the moving average (MA).

The AR involves regressing the variable on its lagged values, whereas the MA part involves modelling the error as a linear combination of error terms occurring at different times in the past.

Depends on the algorithm nature, the possibility to be implemented following the characteristics of each different model.

For example, the Recursive Least Squares is able to work with ARX and with ARMAX.[17] [18] [19]

11.4 IDENTIFICATION BY RECURSIVE LEAST SQUARES

This work implements the famous Recursive Least Squares algorithm to estimate the values of impedance of the capacitor.

Recursive methods are methods which definition is made of itself, in other words, a method is recursive when some of its definitions call other definitions of itself. These kind of methods are widely used in mathematics and computer science to obtain a fast convergence to solutions.

First of all, it is important to know what the Least Squares (LS) method is.

The LS method is an approach to approximate to the solution of overdetermined systems by minimizing the sum of the squares of the residuals made in the results of each equation. LS method is suitable when all the data is available, however it is not appropriate when the task requires to make estimations in real time (called online), since it is not efficient in terms of computational cost to implement the LS algorithm in a repetitive way.

On the other hand, the recursive least squares algorithm (RLS) consists in the recursive application of the LS regression algorithm. Each new data point is taken into account to correct the previous estimation of the parameters from some linear correlation to model the observed system. The method allows for the dynamical application of LS. Same as with LS, there are some correlation equations and several dependent variables.

The RLS algorithm can be defined as an adaptive filter algorithm that recursively finds the coefficients that minimize a weighted linear least squares cost function relating to the input signals. In the derivation of the RLS, the input signals are considered deterministic (there is no randomness associated).

RLS converges extremely fast compared with other methods. Therefore, it is good for estimating the solution of systems with changeable inputs.

This algorithm looks for a covariant matrix (P) that needs to evolve as long as the quantity of samples increases, obtaining a minimized error in the estimation when the quantity of samples is big enough.

The problem comes from the high computational complexity but, RLS filters try to minimize the cost function selecting the coefficients “Wn” well, and updating the filter as new data arrives. A computational benefit that RLS present versus the LS is that there is no need to invert matrices.

The error signal “e(n)” and desired signal “d(n)” are defined in the Figure (19):

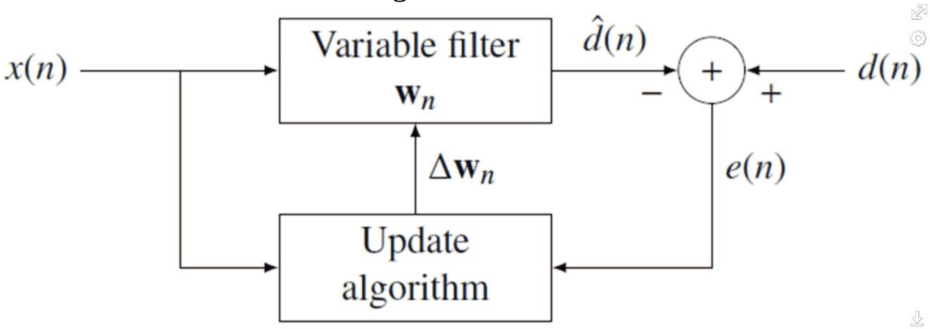

Figure 19. RLS feedback diagram.

The objective is to estimate the parameters of the filter "W", and at each time "n" refer to the current estimate as "Wn" in order to estimate the parameters of the filter the inputs "x(n)" and the error "e(n)" are considered as shown on Figure (19)
Another advantage of the RLS algorithm is that there is no need to invert matrices, thus computational cost is reduced.
The error depends on the filter coefficients through the estimate, like this:

$$e(n)=d(n) - \hat{d}(n) \qquad \text{(Eq.11)}$$

The cost function (Eq. 12) depends on the error and the forgetting factor (λ), the smaller λ is, the less contribution of previous samples to the covariance matrix. This makes the filter more sensitive to recent samples, which means more fluctuations in the filter coefficients (ΔWn), this parameter is delimited by $0 < \lambda \leq 1$, but it usually takes values above 0.95.

$$C\ (Wn) = \sum_{i=0}^{n} (\lambda^{n-i}\, e^2(i)) \qquad \text{(Eq. 12)}$$

11.5 IMPLEMENTATION OF THE RECURSIVE LEAST SQUARES

Initialization of the variables:

p is the filter order

I is the identity matrix of rank p+1,

δ value to initialize P(0)

$$W(n) = 0, \quad \text{(Eq. 12)}$$

$$x(k) = 0, k = -p,....,-1, \quad \text{(Eq. 13)}$$

$$d(k) = 0, k = -p,....,-1, \quad \text{(Eq. 14)}$$

$$P(0) = \delta I, \quad \text{(Eq. 15)}$$

Computation of the RLS for n samples, the number of samples must be big enough for the algorithm to converge to a solution.

$$x(n)= \begin{bmatrix} x(n) \\ x(n-1) \\ x(n-p) \end{bmatrix} \quad \text{(Eq. 16)}$$

$$\alpha(n) = d(n)-x^T(n)w(n-1) \quad \text{(Eq. 17)}$$

Recursive calculation of the gain Vector:

$$g(n)= P(n-1)x(n)\{ \lambda + x^T(n)P(n-1)x(n)\}^{-1} \quad \text{(Eq. 18)}$$

Recursive calculation of the Covariant Vector:

$$P(n) = \lambda^{-1} P(n-1)-g(n)\, x^T(n)\, \lambda^{-1} P(n-1) \quad \text{(Eq. 19)}$$

Recursive calculation of the algorithm filter coefficients:

$$W(n) = w(n\text{-}1) + \alpha(n)g(n) \qquad \text{(Eq. 20)}$$

Implementing the model a new estimation of each parameter per instant of sampling is obtained.[20]

12. IMPLEMENTATION TIME OF THE MODEL TRHOUGHOUT THE DAY

As the ESR and the capacitance does not vary in one day at all, it is not needed to be running the RLS during all day.

Considering the fast convergence of the RLS makes this model interesting to be performed when the voltage and current are not static, that is, when wind speed changes. At that moment, the input data of the model will change. Therefore, some research on how the wind varies throughout the day was done.

The reason that makes the air move from one place to another is the difference of pressure between points. Gases move from high pressure to low pressure areas. This phenomenon happens due to the changes in temperature that are caused by the sun. When gases are warmed up they tend to expand and this is how the differences of pressure are created. As the sun does not warm up the whole planet at the same time, the air moves from the warm places to the cold creating a cycle.

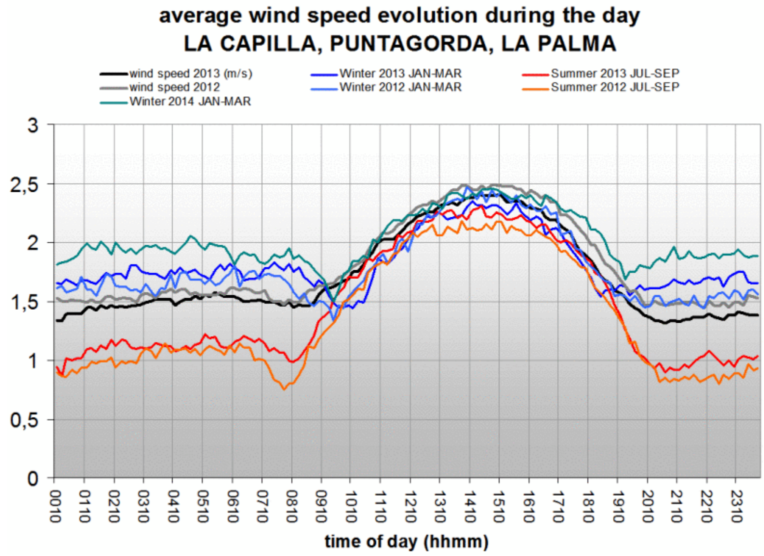

Figure 20. Average wind speed in La Palma [HDmeteo blog]

In Figure (20) the average wind speed throughout the day is compared between different seasons in “La Palma”.

The hours of the day with higher wind speeds are the ones when the sun has the higher warming impact considering the average wind speed in La Palma. This occurs because of the sun effect warming the surface and creating different pressures.

As seen on Figure (20) the lowest wind speed average is before the sunrise and after the sunset. Whereas, the highest wind speed average is between 14 and 15 pm.

Then, if the estimations of the model want to be checked at different times along the day, considering the RLS is a good method when the system input parameters variate, the optimal time would be when the wind speed is changing, as long as it would be when the voltage and current change too.

Thus, running the model at a determined times will allow to make an average to know how the critical values change.

13. MODELLING OF THE SYSTEM

The DC link, where the capacitor is located is going to be the system that will be modelled. Two models are going to be developed, one of them for a RC series as the equivalent circuit of the capacitor, and the other one for RLC series as the equivalent circuit instead of the capacitor.

Basically, the difference between the models is whether the inductance is considered or not.

Both models are going to be tested with theoretical inputs.

13.1 MODELLING OF THE RC SYSTEM

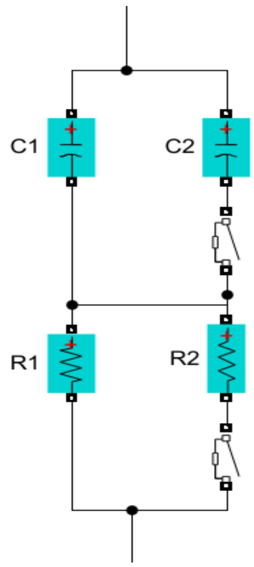

Figure 21. RC circuit diagram

The next calculations were necessary to obtain the results of R and C with the RLS algorithm filter coefficients:

$$\frac{V}{I} = Z = R + \frac{1}{jwC} = R + \frac{1}{sC} = \frac{RsC+1}{sC};$$ (Eq. 21)

Transfer function of first order: $TF = \frac{b0z+b1}{a0-a1z} = \frac{Vdc}{Idc};$ (Eq. 22)

Tustin $s = \frac{2(Z-1)}{T(Z+1)};$ (Eq. 23)

Using the Tustin equation we substitute s:

$$Z(s) = \frac{RC\frac{2(Z-1)}{T(Z+1)}+1}{\frac{2(Z-1)}{T(Z+1)}C} = \frac{RC(2(Z-1)+T(Z+1)}{2(Z-1)C} = \qquad \text{(Eq. 24)}$$

$$\frac{RC(Z-1)+\frac{T}{2}z+T}{(Z-1)C} = \qquad \text{(Eq. 25)}$$

Separating “z” to make it equivalent to $TF = \frac{Vdc}{Idc} = \frac{b0z+b1}{a0-a1z}$; (Eq. 26)

$$= \frac{\left(RC+\frac{T}{2}\right)z+\frac{T}{2}-RC}{(Z-1)C} \qquad \text{(Eq. 27)}$$

Solving:

$$b0=\frac{RC+0{,}5T}{C}; \qquad \text{(Eq. 28)}$$

$$b1=\frac{0{,}5T-RC}{C}; \qquad \text{(Eq. 29)}$$

$$a0=a1=1; \qquad \text{(Eq. 30)}$$

Solving with b0, b1 ,T as variables:

$$C=\frac{2T}{b0+b1}; \qquad \text{(Eq. 31)}$$

$$R=0{,}5b0-0{,}5b1; \qquad \text{(Eq. 32)}$$

, where

“b0” = filter coefficient 0

“b1” = filter coefficient 1

“T” = time

Introducing these formulas in the RLS algorithm, it will iterate giving the estimation of C and R constantly and if the system works properly these parameters should follow the tendency of the real C and R of the capacitor.

As it is observed in Figure (21), samples are used as inputs, as the parametric model used is discrete.

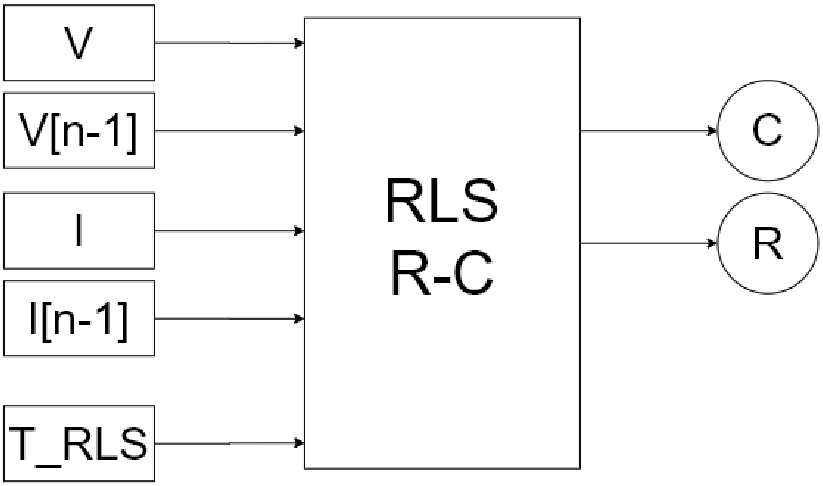

Figure 22. RC model

This is a simple representation of the system. The inputs are at the left, whereas the outputs are found at the right.

For this model, RLS needs as input the samples of Voltage samples [n, n-1], and Current [n, n-1], considering:

$$Z\,(z) = \frac{V(z)}{I(z)} = \frac{b0z+b1}{a0-a1z} = \frac{b0+b1.z^{-1}}{a0+a1.z^{-1}}; \qquad \text{(Eq. 33)}$$

$$I(z)[b0+b1.z^{-1}] = V(z)[\,a0+a1.z^{-1}]; \qquad \text{(Eq. 34)}$$

Therefore:

$$Z\,(n) = \frac{V(n)}{I(n)} = \frac{b0+b1.n^{-1}}{a0+a1.n^{-1}}; \qquad \text{(Eq. 35)}$$

$$I[n]\; b0 + b1.I[n-1] = V[n]\; a0 + a1.V[n-1]; \qquad \text{(Eq. 36)}$$

$$V[n] = \frac{I[n]b0 + b1.I[n-1] - a1.V[n-1]}{a0}; \quad \text{(Eq. 37)}$$

13.2 MODELLING OF THE RLC SYSTEM

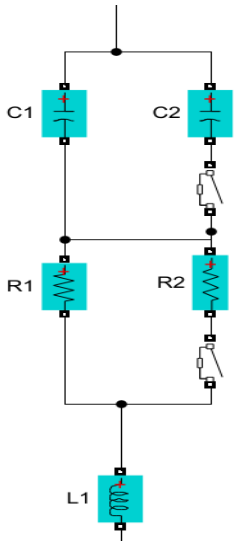

Figure 23. RLC circuit diagram

Following the same procedure as in the RC model:

The next calculations were necessary to obtain the results of R, C and L with the RLS algorithm filter coefficients:

$$\frac{V}{I} = Z = R + \frac{1}{jwC} + jwL = R + \frac{1}{sC} + sL = \frac{RsC + 1 + s^2LC}{sC}; \quad \text{(Eq. 38)}$$

Transfer function of second order:

$$\frac{Vdc}{Idc} = \frac{b0z^2 + b1z + b2}{a0z^2 - a1}; \quad \text{(Eq. 39)}$$

Tustin: $s = \frac{2(Z-1)}{T(Z+1)}$; (Eq. 40)

$$Z(s) = \frac{R\frac{2(Z-1)}{T(Z+1)}C+\frac{2(Z-1)}{T(Z+1)}^{2}LC+1}{\frac{2(Z-1)}{T(Z+1)}C} = \quad \text{(Eq. 41)}$$

$$= \frac{RC(2(Z+1)+4(Z-1)^2CL+T^2(Z+1)^2}{\frac{2(Z-1)}{T(Z+1)}C\,T^2(Z+1)^2} = \quad \text{(Eq. 42)}$$

$$= \frac{2TRC(Z^2-1)+4CL(Z-1)^2+T^2(Z+1)^2}{\frac{2(Z-1)}{T(Z+1)}C\,T^2(Z+1)^2} = \quad \text{(Eq. 43)}$$

$$= \frac{Z^2\left(TRC+\frac{T^2}{2}+2LC\right)+Z(-4LC+T^2)+(-TRC+\frac{T^2}{2}+2LC)}{\mathrm{CT}(Z^2-1)}; \quad \text{(Eq. 44)}$$

Solving:

$$\mathrm{b0}=\frac{TRC+\frac{T^2}{2}+2LC}{CT}; \quad \text{(Eq. 45)}$$

$$\mathrm{b1}=\frac{-4\mathrm{LC}+T^2}{CT}; \quad \text{(Eq. 46)}$$

$$\mathrm{b2}=\frac{-TRC+\frac{T^2}{2}+2LC}{CT}; \quad \text{(Eq. 47)}$$

$$\mathrm{a0}=\mathrm{a1}=1; \quad \text{(Eq. 48)}$$

Solving with b0, b1, b2, T as variables:

$$\mathrm{C}=\frac{2T}{b0+b1+b2}; \quad \text{(Eq. 49)}$$

$$\mathrm{R}=\frac{2}{b0-b2}; \quad \text{(Eq. 50)}$$

$$\mathrm{L}=\frac{T(b0-b1+b2)}{8}; \quad \text{(Eq. 51)}$$

, where

“b0” = filter coefficient 0

“b1” = filter coefficient 1

“b2” = filter coefficient 2

"T" = time

Introducing these formulas in the RLS algorithm, it will iterate giving the estimation of C, R and L continuously and if the system works properly these parameters should follow the tendency of the real C, R and L.

Same as in the previous model, samples are used as inputs, as the parametric model used is discrete.

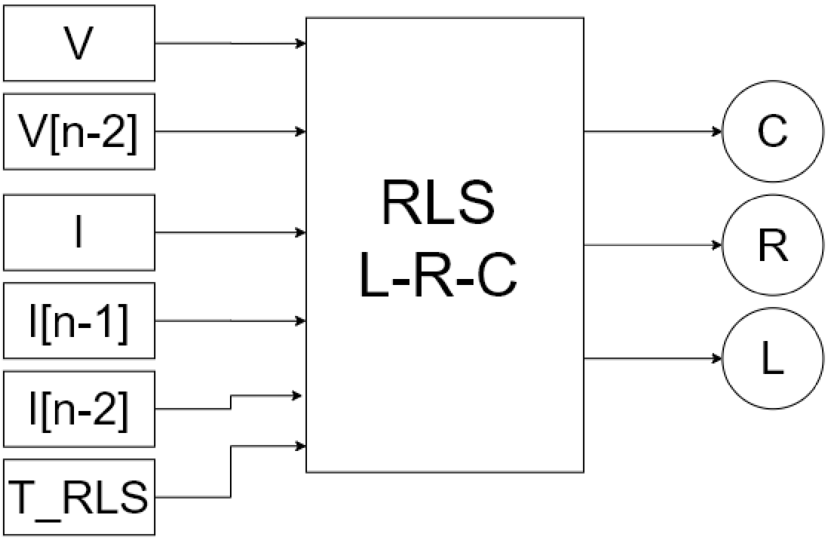

Figure 24: RLC model

This would be graphical representation of the system. The inputs are at the left, whereas the outputs are found at the right.

For this model, the RLS needs as input the samples of Voltage [n, n-2] and Current [n, n-1, n-2], as it is demonstrated below:

$$Z(z) = \frac{V(z)}{I(z)} = \frac{b0z^2+b1z+b2}{a0z^2-a1} = \frac{b0+b1.z^{-1}+b2.z^{-2}}{a0+a1.z^{-2}}; \quad \text{(Eq. 52)}$$

$$I(z)[b0 + b1.z^{-1} + b2.z^{-2}] = V(z)[\,a0 + a1.z^{-2}]; \quad \text{(Eq. 53)}$$

Therefore:

$$Z\ (n) = \frac{V(n)}{I(n)} = \frac{b0 + b1.n^{-1} + b2.n^{-2}}{a0 + a1.n^{-1}};$$ (Eq. 54)

$$b0.\mathrm{I[n]}\ + b1.I[n-1] + b2.I[n-2] = \mathrm{V[n]}\ a0 + a1.V[n-2];$$ (Eq. 55)

$$\mathrm{V[n]} = \frac{\mathrm{I[n]}b0 + b1.I[n-1] + b2.I[n-2] - a1.V[n-2]}{a0};$$ (Eq. 56)

14. SIMULATION VERFICATION

In this part, the simulations with theoretical parameters will be carried out and both models will be tested.

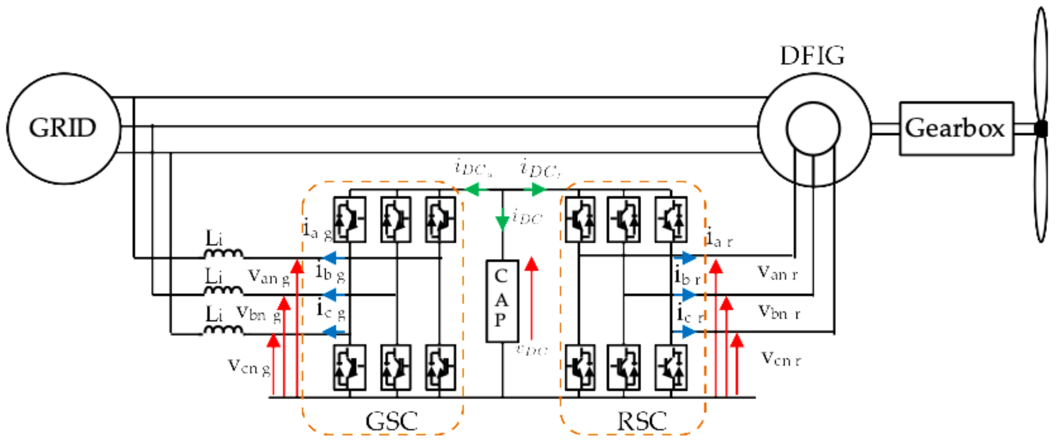

Figure 25. DFIG

In Figure (25) the Double Fed Induction Generator electrical diagram, between both converters we have the DC bus, where the capacitor is located. The rotor converter is at the right side, whereas the grid converter is connected at the left side of the capacitor.

The CAP of Figure (25) was substituted depending on the model as shown in Figure (26) or in Figure (27), in order to consider the ESR of the capacitor and the ESL in the RLC model.

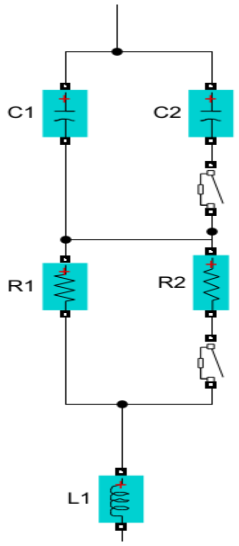

Figure 26. RLC

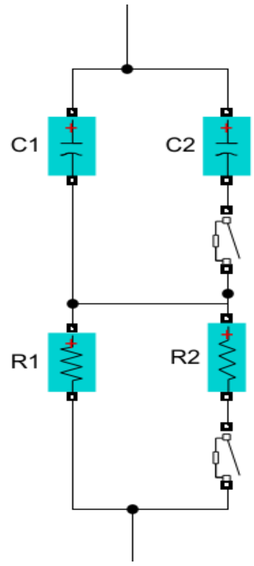

Figure 27. RC

In order to check if the estimation of the resistance or capacitance is good, a resistance or a capacitance, depending on the passive component that want to be checked, is connected in parallel with a switch as seen in Figure (26) and Figure (27).

Having a resistance or capacitance of the same value in parallel, makes the equivalent value of the resistance or capacitance divide by two or double and it is checked if the estimation converges to the new value or not.

To get the theoretical inputs a DFIG was simplified in Simulink, since the important part of the project is the DC link, there was no need to simulate the whole DFIG machine.

Thus, a DC voltage mixed with a sinusoidal signal were applied to the DC link, and the measurements of voltage and current of the DC link were made as it is seen on Figure(28). Those measurements of current and voltage were obtained in real time and introduced in the RLS.

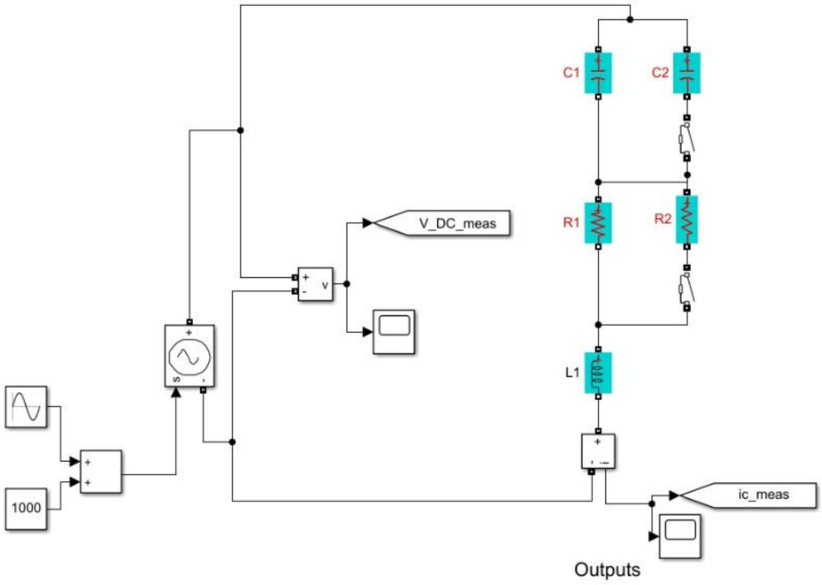

Figure 28. Electrical simplified scheme of the RLC model.

Depending on the frequency in which the RLS is implemented, the estimation precision varies. The higher the frequency of the RLS the faster the convergence to the real value of the parameters estimated. The frequency used is 1 kHz, which is fast enough, as will be seen in the results of simulations, where the estimations converge to the real value in a short period of time.

If the characteristics of the system require a faster convergence, in case the WTG is located in an extremely changing ambient, the frequency of computation of the RLS could be increased.

- ***RC model simulation results:***

PARAMETERS	VALUES
DC Bus Voltage + AC voltage	Vdc = 1000 V + 10 V sin (2 * pi * 500*t)
Capacitor ESL	0 H
Capacitor ESR	1e-3 Ω

Capacitor C	0.1 F
RLS frequency	1 kHz
RLS forgetting factor	λ RLS = 0.995

Table 1. Parameters used in RC model simulations.

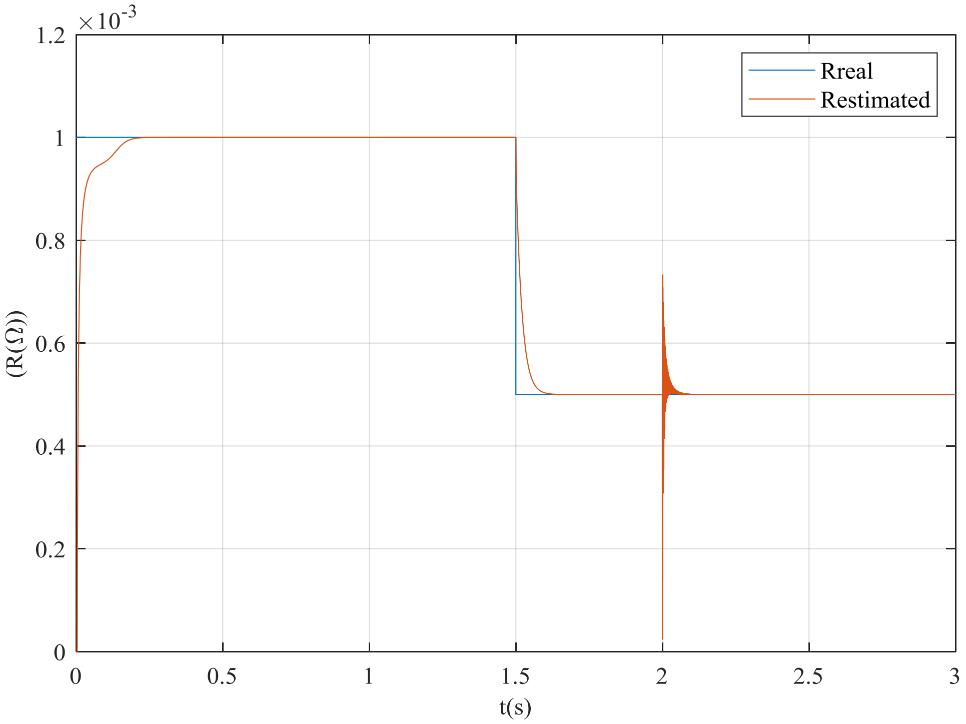

Figure 29. Resistance estimation

As it is seen in the Figure (29) at second 1.5 when the switch makes contact the real resistance becomes half and the estimation converges to that value.

The RLS has some noise when the equivalent capacitance of the circuit doubles, but it is seen how it converges to the proper value again.

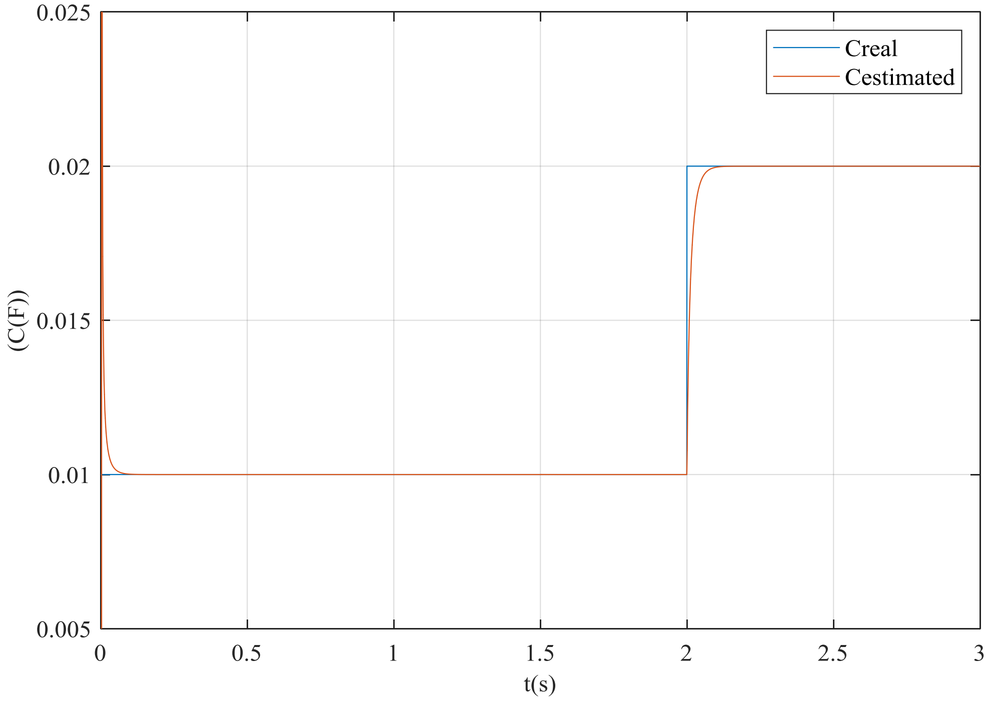

Figure 30. Capacitance estimation

With the capacitance it happens the same, in the Figure (30) it is shown how at second two, when the real capacitance becomes double, the estimation converges to that value. However, on this case there is no notice of change when the equivalent resistance is divided by two.

- ***RLC model simulation results:***

The difference with the RC model is the L. In this case, a very small inductance is placed in series with the R and the C and estimated, however no inductance is added in parallel, so the value of the inductance is not changing along the simulation. Whereas the R and the C will work in the same way as in the RC model, placing a Resistance and a Capacitance in parallel to make a change in the values and see like that, how the algorithm converges to the new value.

PARAMETERS	VALUES
DC Bus Voltage + AC voltage	Vdc = 1000 V + 10 V sin (2 * pi * 500*t)
Capacitor ESL	0 H
Capacitor ESR	1e-3 Ω
Capacitor C	0.1 F
RLS frequency	1 kHz
RLS forgetting factor	λ RLS = 0.995

Table 2. Parameters used in RLC model simulations.

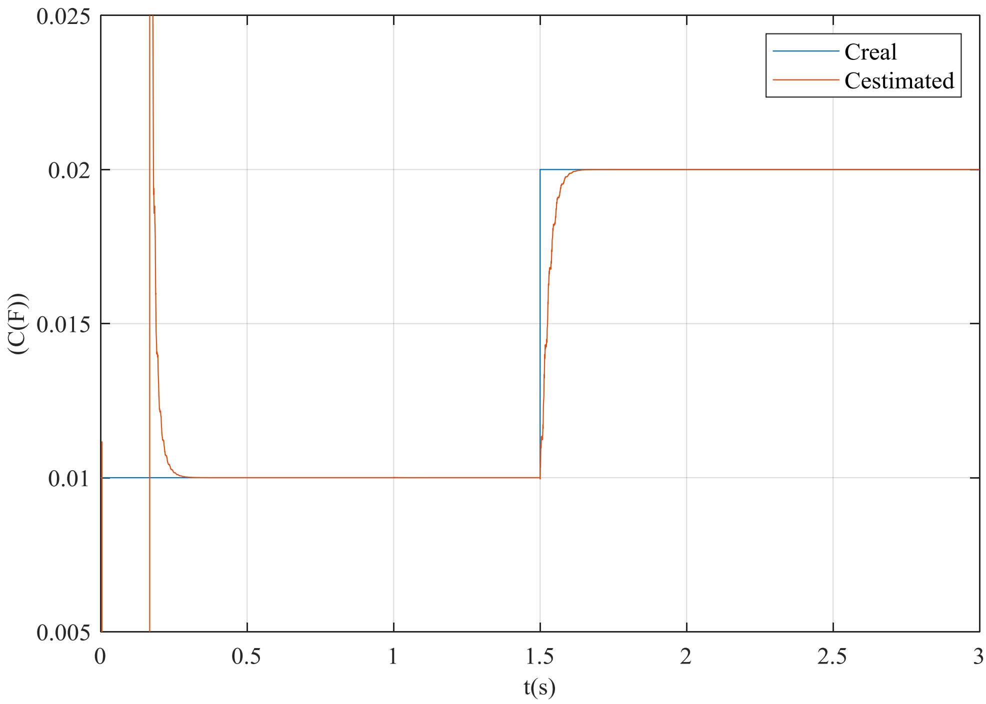

Figure 31. Capacitance estimation

In this graph, the estimated capacitance is compared with the real one. At the beginning, it takes around 0.3 seconds to the algorithm to reach to the real value. At the instant 1.5 a capacitor is added in parallel to the first one, and the algorithm takes around 0.1 seconds reaching the proper value of the estimation. When the resistance is added at the instant 1, the estimation of the capacitance is not disturbed.

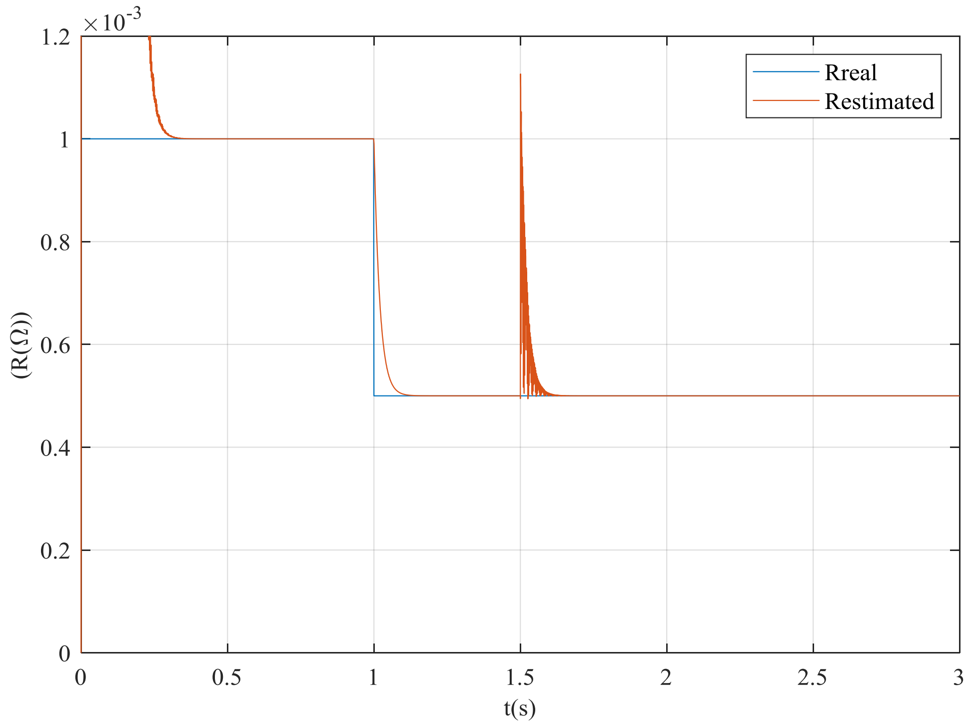

Figure 32. Resistance estimation

In Figure (32), the estimation of the resistance is compared with the real value. At the instant 1, a resistance is added in parallel to the other one as it is shown in Figure (25). It is appreciated that the estimation reaches the real value extremely fast after the resistance equivalent value divides by two. Notice that when the capacitance is added at the instant 1.5 there is a disturbance in the resistance estimation.

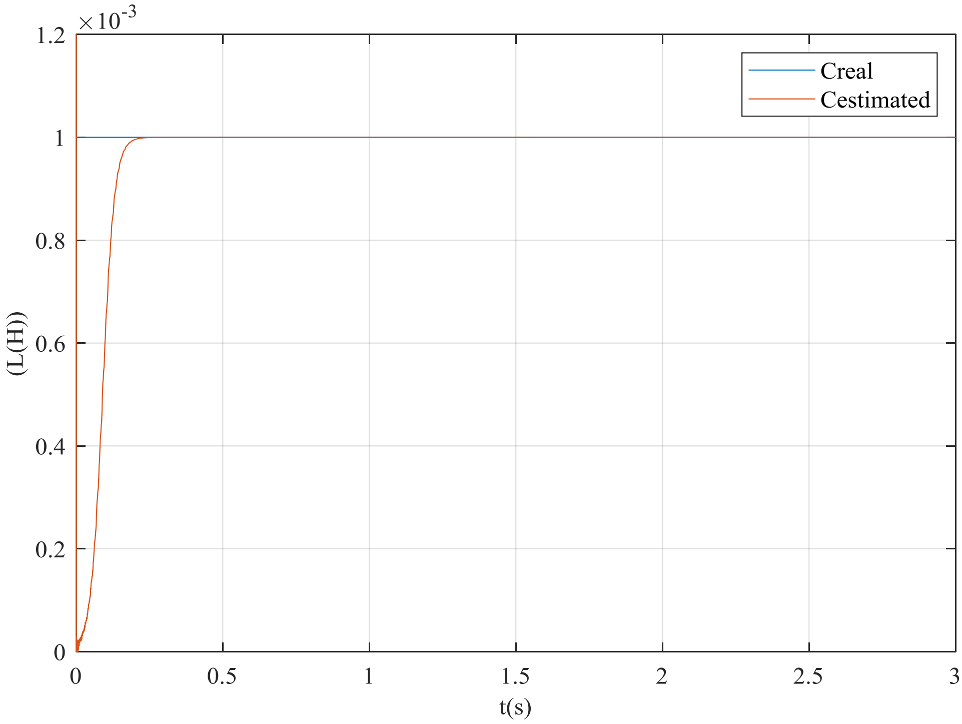

Figure 33. Inductance estimation

The inductance is estimated and compared to the real one, as it is seen it converges to the real one in 0.3 seconds.

After these simulations, it was verified that both models worked and therefore the experimental part was carried out.

15. EXPERIMENTAL RESULTS

In this part, a DFIG was used to obtain real measured data of the DC link and be able to implement the model with real data.

PARAMETERS	**VALUES**
Rated Power	Sg = 1.5 MVA
DC Bus Rated Voltage	Vdc = 1150 V
Rated Wind Speed	11 m/s
Grid-Side Converter switching frequency	Fgsc = 5 kHz

Rotor-Side Converter switching frequency	Frsc = 2.5 kHz
Grid-side inductance	Lg = 0.16 mH
Capacitor ESL	0 mH
Capacitor ESR	1.2e-3 mΩ
Capacitor C	420 µF
Measuring Frequency	1 MHz
RLS frequency	1 kHz
RLS forgetting factor	λ RLS = 0.995

Table 3: Parameters of the experimental part.

The following images show the set-up of the experiment:

Figure 34. Experimental set-up

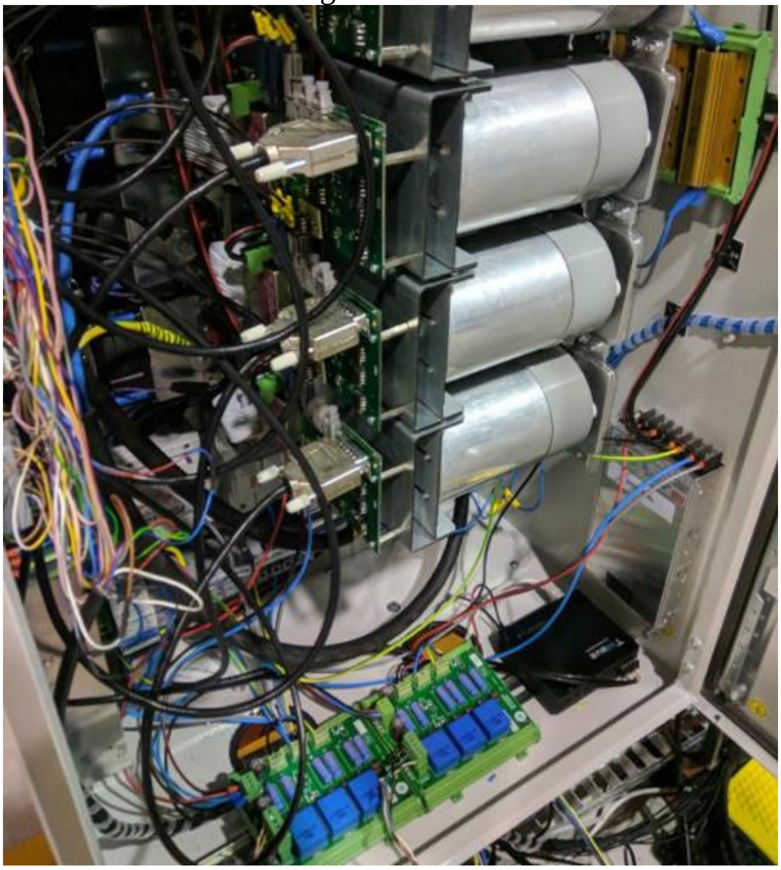

Figure 35. Experimental set-up

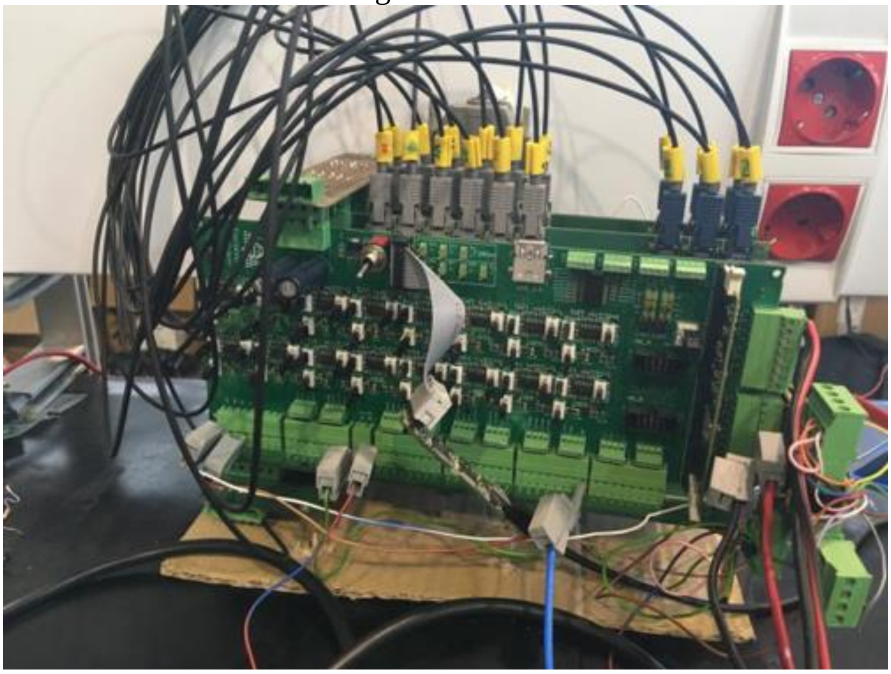

Figure 36. Experimental set-up

The current, voltage and time were measured at the capacitor of the B2B that is part of the DFIG.

The voltage and the current during the experiments were constant simulating constant wind and keeping the generator working in a static mode, obviously there was a little bit of error in the measurements.

It was not the ideal experimental data for checking the model, because as was seen in [11.4 IDENTIFICATION BY RECURSIVE LEAST SQUARES] it works better when the system inputs are changing.

The capacitor used for the experimental part had the following characteristics:

- Capacitance = 420 µF
- Resistance = 1.2e-3 mΩ

As long as the capacitor used had negligible inductance, it was of the order of “nH”, it was decided not to estimate the inductance associated to the capacitor. Thus, the RC model will be implemented.

Anyway, if another capacitor with higher inductance was used, the procedure would be simply changing the RLS algorithm to the one of the RLC model instead of the RC.

Once all data was collected, everything is ready to start to prepare the model to get the estimations for the real input data.

The difference between the experimental part and the theoretical part comes from the input data of the system. As long as experimental values are used, some changes must be done so as to adapt the input data in the RLS.

First, a lowpass filter was implemented in order to filter the data. The filter used was a second order filter where the low pass frequency was 2500 Hz.

Considering the measuring frequency of the experimental data was 1MHz and the frequency of the RLS algorithm was 1 kHz, another filter is needed to get same frequency. Thus, a way to take one per one hundred measured data in Matlab was created, obtaining both frequencies equal. The data was resampled to the frequency of the RLS after the lowpass filter.

Once the input data was filtered and resampled to the frequency of the RLS, the input data for the model is ready.

Then, a "for" loop will be implemented to iterate the RLS algorithm for each data along the experimental data length.
The results obtained are plotted in a graph compared with the real data:

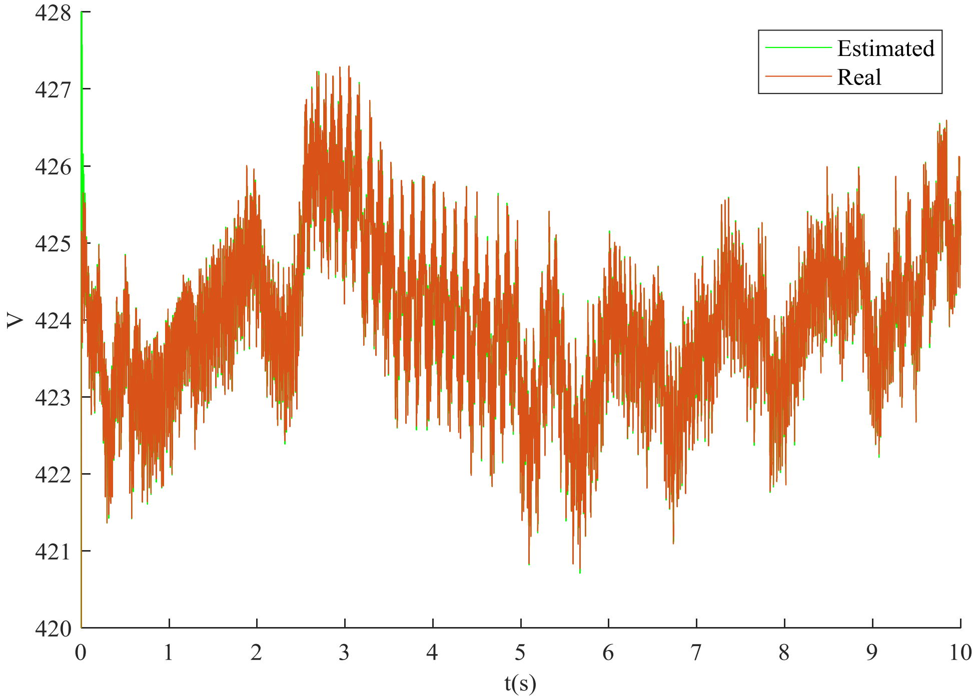

Figure 37. Vreal vs Vestimated

In Figure (37), the green line is the estimated voltage and the brown the measured one. No error is appreciable at all as long as the estimated line is covered by the brown one almost during the entire time domain, except for the first instants, but anyway the convergence was extremely fast. In order to appreciate the Voltage error better another graph was plotted.

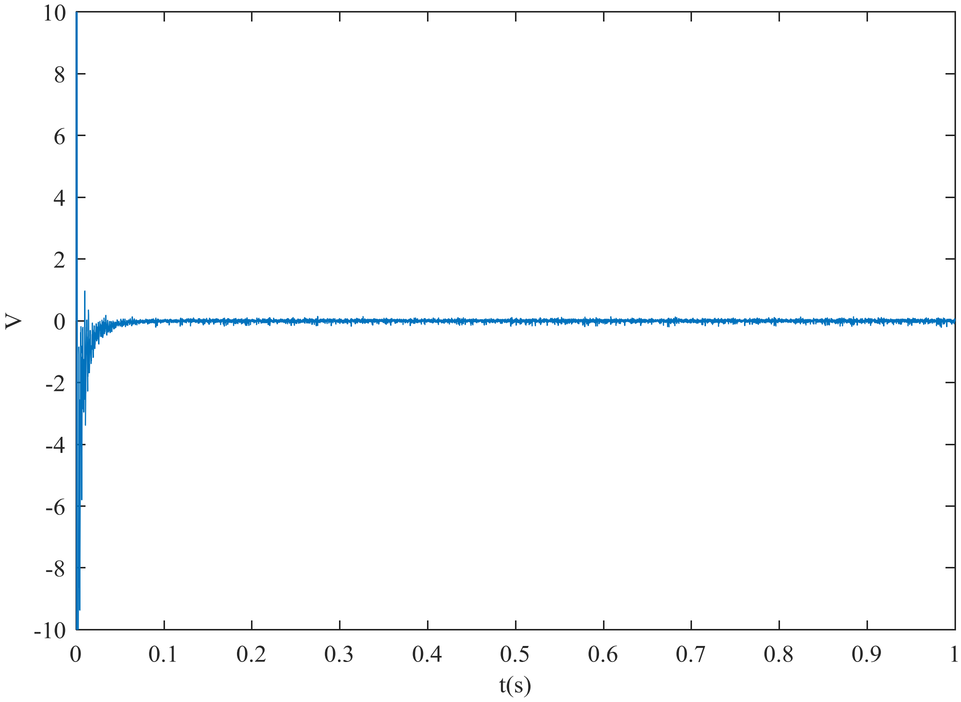

Figure 38. Voltage error between the estimation and the real one

In Figure (38) the blue line is (V real - V estimated) it is seen with a better degree of detail for the first second of simulation. It takes less than 0.1 seconds to converge to the real value. The error is almost null from that time on, taking into account the magnitude of the voltage is over 400 Volts.

Now the resistance estimation will be plotted:

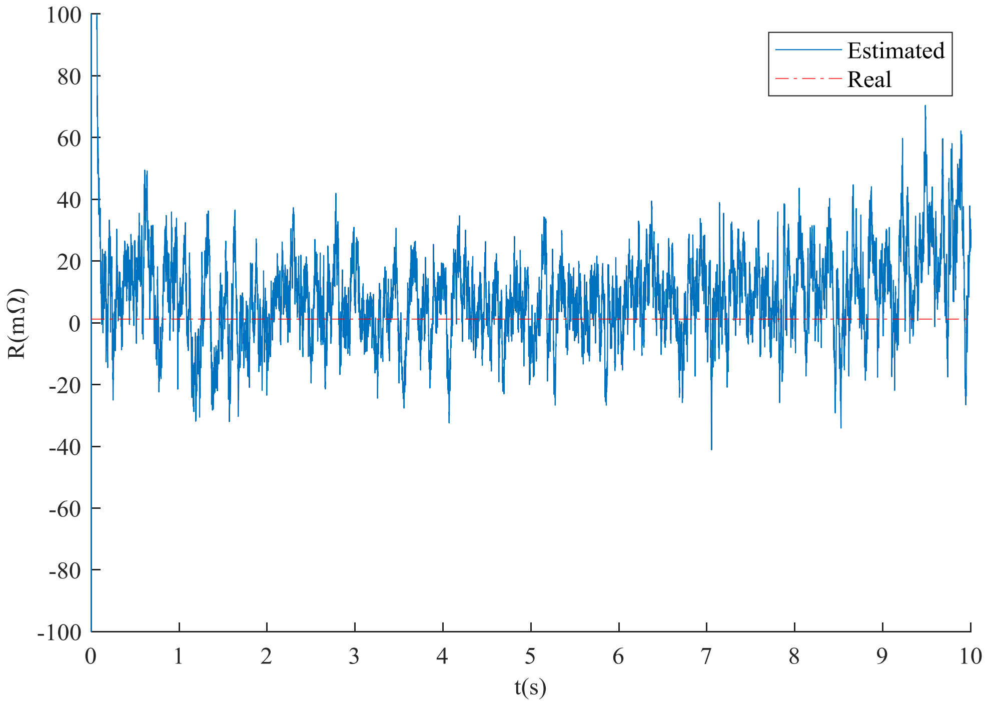

Figure 39. Resistance estimation compared with the real ESR of the capacitor.

The results as it is seen in the y-axis are in mΩ, it is quite hard to have an extremely precise estimation of the real ESR, due to the fact a wire was needed to make the measurements and the ESR is not a big resistance so the resistance of the wire is disturbing the results.

However, what really matters is the tendency of the estimations during the lifetime of the capacitor. So, it is important to make an average of the estimations made during some time in order to compare that with the new average made after one month, for example. It is important to keep the data from the first day of operation, when the capacitor is new, obtaining like this the initial ESR, and be able to see the tendency of this value and compare the results obtained with the information of [9.2 CRITICAL VALUES OF CAPACITORS].

The capacitance estimation is now plotted:

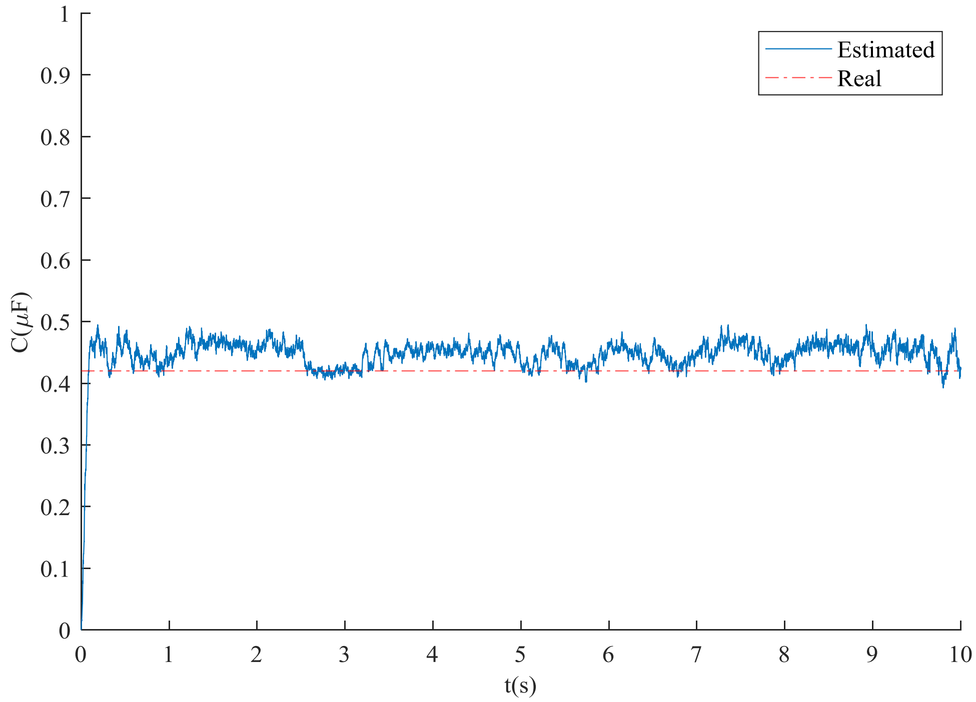

Figure 40. Capacitance estimation compared with the real capacitance of the capacitor.

In Figure (40), there is a little bit of error too between the real capacitance and the estimated one.

Same process as for the resistance should be followed.

Keep all estimations data from the first moment of work of the capacitor, in order to see the tendency of the capacitance estimation, doing an average of a big quantity of samples of data before getting to any conclusion.

The capacitance should be compared with the critical values seen in [9.2 CRITICAL VALUES OF CAPACITORS] in order to make the replacement and reduce as much as possible the downtime of wind turbines.

After the experimental part, it is concluded the model seem to work as it did for the theoretical simulations and could be implemented in a real DFIG machine.

16. COST OF THE PROJECT

<u>Development cost:</u>

MATLAB licence 1 year: 968 euros, price including VAT.

600 hours of engineering:

$$600 \text{ x } 10.64\text{ €} = 6{,}384\text{€} \quad \text{(Eq. 57)}$$

Considering tests, development of algorithm, simulations, etc…

<u>Material cost (Material for tests not included):</u>

In order to implement this work into a turbine the materials needed are the following:

-Voltmeter to measure the voltage of operation.

-Hall Sensors to check the current. (The cost depends on the size of the WTG)

-Microcontroller able to implement the RLS with the measured data and to keep in memory (non-volatile memory like (EEPROM)) the RLS estimations until the end of capacitor´s life to be able to check the tendency of the estimations.

-The microcontroller must have a WIFI or similar communication protocol to let the maintenance company be aware of the estimations tendency.

Possibly all these materials are not needed as the WTG already measures voltage and currents and already has a control unit, which has the characteristics mentioned, so the cost, would be reduced to the development of the algorithm hours and the Matlab license.[21]

$$\text{Total cost} = 968 + 6{,}384 = 7352 \text{ euros} \quad \text{(Eq. 58)}$$

17. CONCLUSION AND FUTURE WORKS

Taking into account the results of the experiments, it is concluded that the model works. This method could be used to do a preventive maintenance of the capacitors of DFIG.

The fact of knowing the state of power capacitors is interesting but not just applied in wind turbines, but also applied in any power conversion.

Next works with this model will be done in order to do a predictive maintenance in different power converters applications.

It could be also interesting to use this kind of application in the power converters in some applications where humans are involved directly, considering, nowadays power converters are used much more, because electricity powers almost everything.

Obviously, this is a remote situation, but it might even help to save some life in case there is a sudden failure of the power converter of an electric car due to a capacitor failure. That car might be in a risky situation where the throttle is necessary, and if there is no power conversion the car is not able to speed up.

18. BIBLIOGRAPHIC REFERENCE

[1] A special report on global exposure to air pollution and its disease burden. https://www.stateofglobalair.org/sites/default/files/soga_2019_report.pdf

[2]Red eléctrica España
https://www.ree.es/en/press-office/news/press-release/2019/12/spain-closes-2019-10-more-installed-renewable-power-capacity

[3] Wind energy in Europe in 2019 - Trends and statistics https://windeurope.org/wp-content/uploads/files/about-wind/statistics/WindEurope-Annual-Statistics-2019.pdf

[4] Mohamad, Azizul & Amin, N.A.M. & Tee, TOH & Abdul Majid, M.S. & Daud, Ruslizam. (2014). Review of Analysis on Vertical and Horizontal Axis Wind Turbines. Applied Mechanics & Materials. 695. 10.4028/www.scientific.net/AMM.695.801.

[5] Arshad, Muhammad & O'Kelly, Brendan. (2013). Offshore wind-turbine structures: A review. Proceedings of the Institution of Civil Engineers – Energy. 166. 139-152. 10.1680/ener.12.00019.

[6] Solar PV and Wind Energy Conversion Systems, S. Sumathi, L.Ashok Kumar, P.Surekha

[7] Arnau, Carles & Dòria-Cerezo, Arnau & Fossas, Enric & Gaviria, César & Griñó, Robert. (2004). GEOPLEX: Back-to-back converter for an electrical machine application.

[8] Pena R., Clare J. & Asher G. M. “Doubly fed induction generator using back-to-back PWM converters and its application to variable speed wind-energy generation” IEE Proceedings Electric Power Applications 1996. 143(3) 231–241p

[9] Qiu, Yingning & Zhang, Wenxiu & Cao, Mengnan & Feng, Yanhui & Infield, David. (2015). An Electro-Thermal Analysis of a Variable-Speed Doubly-Fed Induction Generator in a Wind Turbine. Energies. 8. 3386-3402. 10.3390/en8053386.

[10] John Fletcher and Jin Yang (2010). Introduction to the Doubly-Fed Induction Generator for Wind Power Applications, Paths to Sustainable Energy, Dr Artie Ng (Ed.), ISBN: 978-953-307-401-6, InTech, Available from: http://www.intechopen.com/books/paths-to-sustainable-energy/introduction-to-the-doubly-fed-inductiongenerator-for-wind-power-applications

[11] Qiu, Yingning & Zhang, Wenxiu & Cao, Mengnan & Feng, Yanhui & Infield, David. (2015). An Electro-Thermal Analysis of a Variable-Speed Doubly-Fed Induction Generator in a Wind Turbine. Energies. 8. 3386-3402. 10.3390/en8053386.]

[12] Pavol, Špánik & Frivaldsky, Michal & Kanovsky, Andrej. (2014). Life time of the electrolytic capacitors in power applications. 233-238. 10.1109/ELEKTRO.2014.6848893.

[13] Kulkarni, Chetan & Biswas, Gautam & Koutsoukos, X. & Goebel, Kai & Celaya, Jose. (2010). Physics of Failure Models for Capacitor Degradation in DC-DC Converters.

[14]Kemet, Electronic components (Aluminium Electrolytic Capacitor datasheet) https://content.kemet.com/datasheets/KEM_A4081_ALC70.pdf

[15] Cooling approaches for high power inverters. White Paper WP083022EN, Chris Thompson Eaton

[16] Zhou, Dao & Blaabjerg, F. & Lau, Mogens & Tonnes, Michael. (2013). Thermal profile analysis of Doubly-Fed induction generator based wind power converter with air and liquid cooling methods. 2013 15th European Conference on Power Electronics and Applications, EPE 2013. 1-10. 10.1109/EPE.2013.6631992.

[17] Arafet Padilla, Pedro y otros. 2008. Métodos de Identificación dinámica. [En línea] Facultad de Ingeniería Eléctrica. Universidad de Oriente., Junio de 2008. [Citado el: 19 de Octubre de 2016.] https://www.researchgate.net/profile/Pedro_Arafet_Padilla/publication/242121057_Metodos_de_Identificacion_dinamica/links/55549f8408ae980ca609f977/Metodos-de-Identificacion-dinamica.pdf.

[18] Åström, K. J. y Eykhoff, P. 1971. System Identification: A survey. Automatica, Vol. 7, pp. 123-162. [En línea] 1971. [Citado el: 19 de Octubre de 2016.] http://www.control.lth.se/documents/1971/ast71.pdf.

[19] Chica Leal, Alonso & Rey, F. & Aristizabal, Andres. (2012). Application of autoregressive model with exogenous inputs to identify and analyse patterns of solar global radiation and ambient temperature. International Journal of Ambient Energy. 10.1080/01430750.2012.686197.

[20] L. Ljung, System Identification: Theory for the User. Upper Saddle River, NJ, USA: Prentice-Hall, Inc., 1986.

[21] Matlab license: https://es.mathworks.com/pricing-licensing.html